Improving the Reliability of Ultrasound Evaluation of Articular Cartilage for Clinical Applications

Keisuke YAMADA

Table of Contents

Chapter 1
General Introduction

1.1 Ultrasound measurement of articular cartilage

Articular cartilage exists in synovial joint covering the end of bone. It provides a nearly friction-free load-bearing joint surface so that humans can make the joint movements smooth and pain-free. However, articular cartilage can be damaged by trauma or inflammatory disease, and osteoarthritis (OA). OA is the most common form of arthritis. During the progression of OA, changes in the cartilage structure and composition, in morphologic features, and in mechanical properties occur. Once articular cartilage is damaged, the cartilage is not restored to its normal state because of its limited capacity for repair [1, 2]. As the common treatment of severe OA, artificial joint replacement surgery is performed. However, the life of artificial joint is limited and a second surgery is more difficult [3].

Recently, many new therapies to regenerate the cartilage such as cultured chondrocyte or tissue-engineered cartilage transplantations are studied for the treatment of cartilage defects [4]. Therefore, in vivo evaluation of regenerate cartilage is required to compare the effects of the regeneration methods. However, the clinical diagnostic methods of articular cartilage such as X-ray or joint arthroscopy can only detect the large defect of cartilage or change in shape of subchondral bone, and the evaluations are not quantitative.

For quantitative evaluation of articular cartilage, Hattori et al. developed the evaluation

system using ultrasound. In the ultrasound evaluation system, the probe which has a small ultrasound transducer on the head is introduced into the joint with arthroscopy. The echogram from cartilage is used for evaluations, the elasticity of cartilage is evaluated with echo amplitude from cartilage surface, and thickness of cartilage is evaluated with time interval between the echoes from cartilage surface and from subchondral bone. Previous study reported that the ultrasound evaluation system could predict the histological characteristics of OA cartilage and tissue-engineered cartilage. This method has been used to assess living human cartilage [5-10].

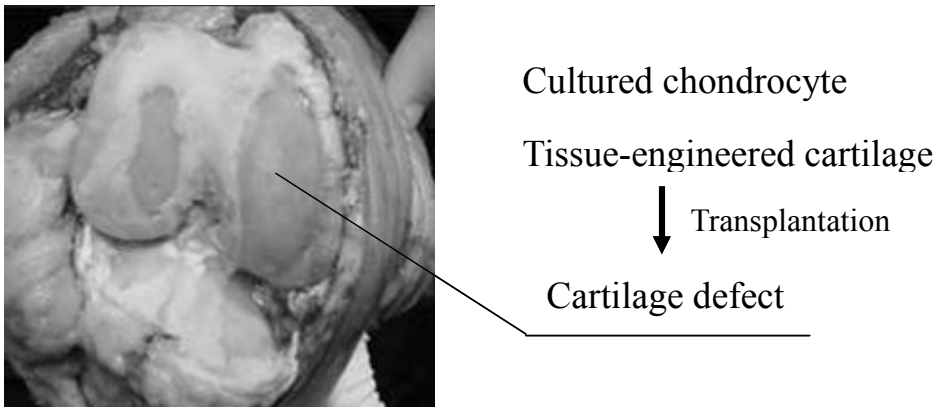

Figure 1.1 The photograph of OA joint and cartilage defect. The transplantations of cultured chondrocyte or tissue-engineered cartilage are studied for the treatment of cartilage defect.

(a) X-ray imaging

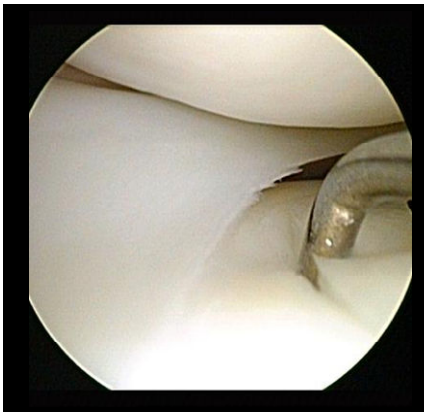

(b) Arthroscopy and probing

Figure 1.2 The clinical diagnostic methods of articular cartilage. (a) The X-ray imaging of the knee joint. (b)

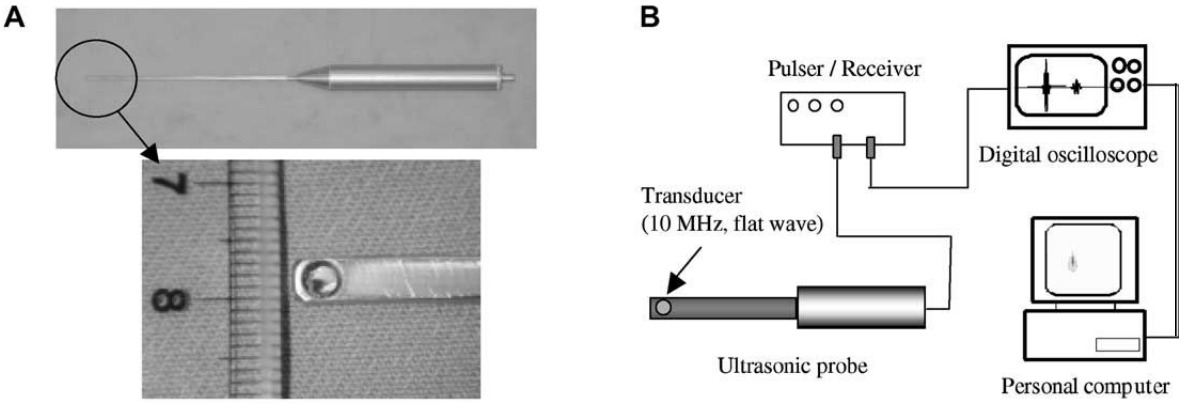

Figure 1.3 The ultrasound evaluation system of articular cartilage. (A) Ultrasonic probe to use in clinical practice. (B) Schematic illustration of the cartilage evaluation system [6].

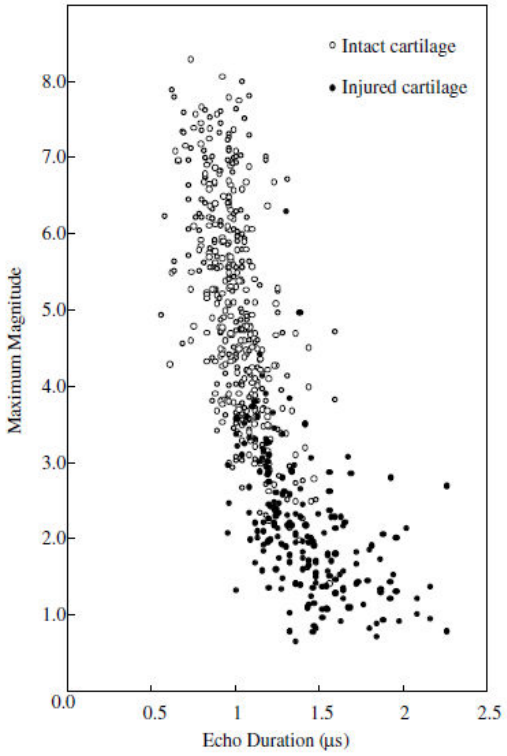

Figure 1.4 Results of ultrasound measurement obtained from living human cartilage under arthroscopy [6].

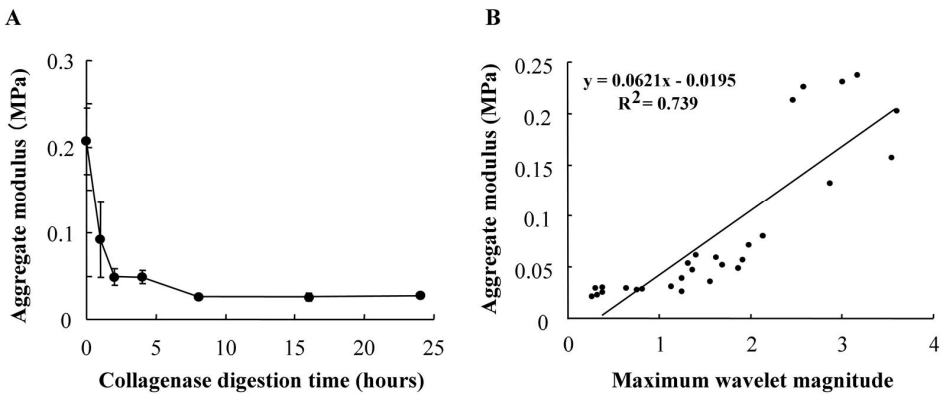

Fugure 1.5 Time-course of aggregate modulus in collagenase-digested articular cartilage (A) and the relationship between maximum wavelet magnitude and aggregate modulus (B) [11].

1.2 Theme of thesis

The ultrasound measurement provided a quantitative and noninvasive evaluation of articular cartilage. However, the ultrasound method has the following problems from the point of view of the accurate measurement in clinical use.

1. Error in the cartilage thickness measurement.
2. Lack of the angle index of ultrasound probe.
3. Unconscious avoidance of degenerated area.
4. Mismatch between cognition and reality of probe state.
5. Lack of the evaluation of the anisotropy of articular cartilage.

This study is expected to improve the reliability of the ultrasound evaluation of articular cartilage by resolving these problems. For the accurate measurement of cartilage thickness, the effectiveness of estimation of sound velocity using echo reflectance ratio was evaluated in chapter 2. For the support of alignment of probe angle, “Rise-to-Peak time” was proposed as an index of probe angle in chapter 3. For suppression of unconscious avoidance of degenerated area, the effectiveness of the display of the “Rise-to-Peak time” to the operator in the ultrasound measurement was evaluated using “Acceptance” in chapter 4. For the evaluation of the mismatch between the cognition and the reality in ultrasound measurement, a user test was performed in chapter 5. For the development of the nondestructive method to evaluate the anisotropy of articular cartilage, the effectiveness of measurement of shear wave speed using surface wave was investigated in chapter 6.

1.3 Reference

[1] Mankin, H.J., Dorfman, H., Lippiello, L., Zarins, A., Biochemical and metabolic abnormalities in articular cartilage from osteo-arthritic human hips, Journal of Bone and Joint Surgery, Vol. 53, (1971), pp. 523-537

[2] Buckwalter, J.A., Mankin, H.J., Articular cartilage. Part II: Degeneration and osteoarthrosis, repair, regeneration, and transplantation, Journal of bone and joint surgery, Vol. 79, (1997), pp. 612-632

[3] Shibata, N., Kurtz, S.M., Tomita, N., Recent advances of mechanical performance and oxidation stability in ultrahigh molecular weight polyethylene for total joint replacement: highly crosslinked and α-tocopherol doped, Journal of Biomechanical Science and Engineering, Vol. 1, (2006), pp. 107-123

[4] Temenoffa, J.S., Mikos, A.G., Review: tissue engineering for regeneration of articular cartilage, Biomaterials, Vol. 21, (2000), pp. 431-440

[5] Hattori, K., Mori, K., Habata, T., Takakura, Y., Ikeuch, K., Measurement of the mechanical condition of articular cartilage with an ultrasonic probe: quantitative evaluation using wavelet transformation, Clinical Biomechanics, Vol. 18, (2003), pp. 553-557

[6] Hattori, K., Takakura, Y., Ishimura, M., Habata, T., Uematsu, K., Ikeuch K., Quantitative arthroscopic ultrasound evaluation of living human cartilage, Clinical Biomechanics, Vol.19, (2004), pp. 213-216

[7] Hattori, K., Takakura, Y., Morita, Y., Takenaka. M., Uematsu. K., Ikeuchi. K., Can ultrasound predict histological findings in regenerated cartilage?, Rheumatology, Vol.43, (2004), pp. 302-305

[8] Hattori, K., Takakura, Y., Ohgushi, H., Habata, T., Uematsu, K., Takenaka, M., Ikeuchi, K., Which cartilage is regenerated, hyaline cartilage or fibro cartilage? Non-invasive ultrasonic evaluation of tissue engineered cartilage, Rheumatology, Vol. 43, (2004), pp. 1106-1108

[9] Hattori, K., Takakura, Y., Tanaka, Y., Habata, T., Habata, T., Kummai, T., Uematsu, K., Sugimoto, K., Ikeuchi, K., Quantitative ultrasound can assess living human cartilage, The Journal of Bone & Joint Surgery, Vol. 88, (2006), pp. 201-212

[10] Kuroki, H., Nakagawa, Y., Mori, K., Ohba, M., Suzuki, T., Mizuno, Y., Ando, K., Takenaka, M., Ikeuchi, K., Nakamura, T., Acoustic stiffness and change in plug cartilage over time after autologous osteochondral grafting: correlation between ultrasound signal intensity and histological score in a rabbit model, Arthritis Research & Therapy, Vol. 6, (2004), pp. 492-504

Chapter 2

Correction of Thickness Measurement by Ultrasound for Articular Cartilage Using Sound Velocity Estimation

2.1 Introduction

Ultrasound has been widely used in clinical practice for the noninvasive evaluation of soft tissues. In addition to shape, movement, alteration, and integrity of tissues can also be observed in real time. However, the ultrasound measurement of shape is not sufficiently accurate if constant sound velocity is used. For example, information about cartilage thickness [1, 2, 3] is altered by the change in sound velocity from cartilage degeneration [4, 5].

The aim of this study was to estimate sound velocity using surface echo reflectance. As a first stage for evaluating the clinical relevance of this method, the error of the cartilage thickness measurement was determined using collagenase-treated osteochondral plugs as a model of osteoarthritis (OA).

2.2 Material and method

2.2.1 Preparation of cartilage samples

Osteochondral plugs (diameter 5 mm; n=30) were excised from a flat area of the trochlea femoris of frozen porcine knee joints. The osteochondral samples were

removed from the subchondral bone using a microtome and the bottom was shaped parallel to the surface.

2.2.2 Enzyme treatment

The osteochondral samples (n=20) were digested in phosphate-buffered saline (PBS; Invitrogen Corp., Carlsbad, CA, USA) containing 30 U/ml collagenase type II at 37°C (Worthington Biochemical Corp., Lakewood, NJ, USA) for 4 and 9 hours (4 h and 9 h groups, respectively). Ten osteochondral samples in PBS alone at 37°C were used as controls (0 h group).

2.2.3 Ultrasound measurement

Figure 2.1 shows the ultrasound evaluation system for articular cartilage. The system consisted of a personal computer, a digital oscilloscope, a pulsar/receiver, and a transducer (the ultrasonic probe) (XMS-310, Panametrics Japan Co., Ltd., Tokyo, Japan). The transducer emits and receives the ultrasound wave. A plane wave with a central frequency of 10 MHz is oscillated from the transducer. Reflected wave was received by the transducer and recorded by the oscilloscope. The sampling frequency was 500 MHz. The specimen was fixed on a stage in saline using bond, and the transducer was placed perpendicular to the surface of sample. Figure 2.2 shows a typical ultrasonic echogram demonstrating echo peaks from the surface and bottom of the specimen. Perpendicularity between the transducer and the cartilage surface was ensured by gently aligning the stage angle to obtain the maximum echo amplitude. The measurement was also performed with stainless steel as a specimen and the amplitude of echo from the surface was obtained.

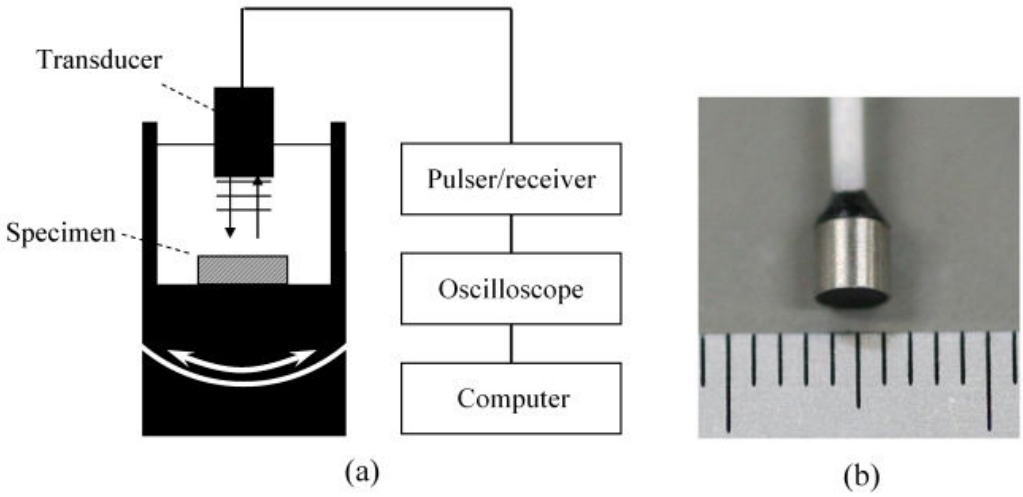

Figure 2.1 (a) Schematic drawing of ultrasound measurement system. A small transducer was fixed over the measurement device. Measurement was performed in saline at room temperature and A-mode echogram was measured. (b) Ultrasound transducer (diameter: 2 mm; frequency: 10 MHz).

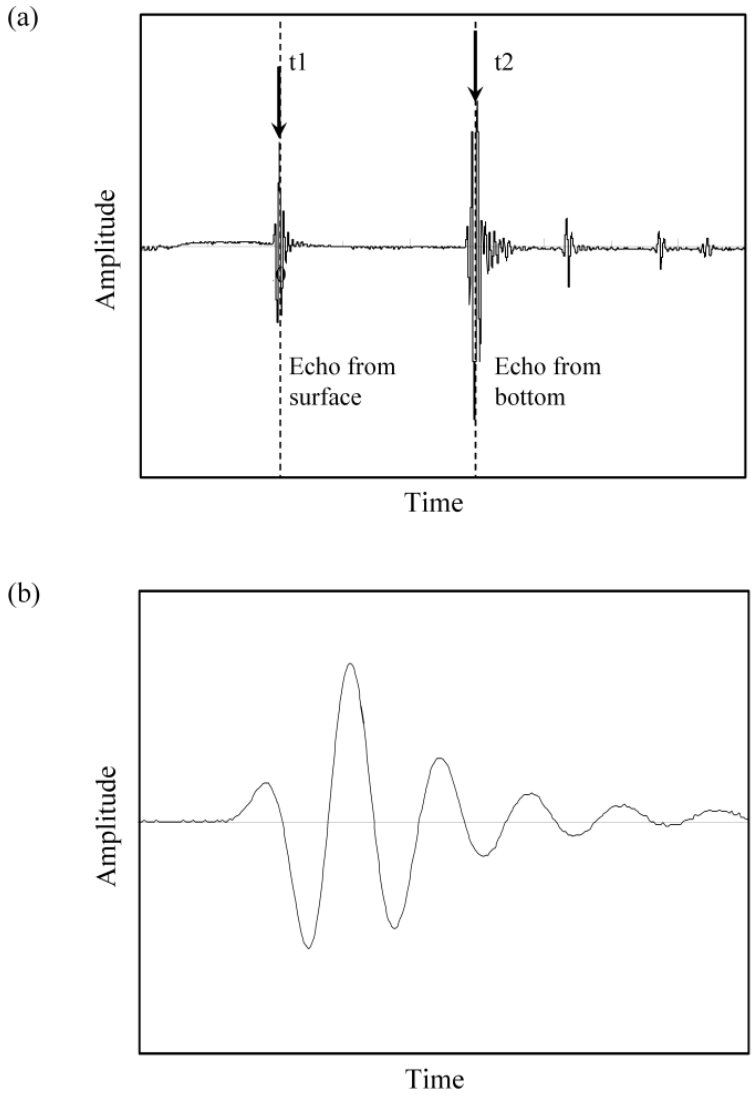

Figure 2.2 Typical waveform of ultrasound echo. (a) Echoes from the surface and bottom of a specimen were recorded. The times to peak amplitude were recorded as t1 and t2. (b) Enlarged waveform of echo from surface of specimen.

The reflectance ratio was calculated from the equation:

$$R_c = \frac{A_c}{A_s} R_s \tag{2.1}$$

where *As* and *Ac* are the maximum peak-to-peak echo amplitudes recorded from stainless steel and cartilage surfaces, respectively. *Rs* and *Rc* are the reflectance ratio of the steel–water and cartilage–water interfaces. In this study, *Rs*=0.936 [6] was used as the reflectance ratio of the steel–water interface.

2.2.4 Calculation of sound velocity

Sound velocity in articular cartilage was calculated from the reflectance ratio as follows:

$$c_c = \frac{1+R_c}{1-R_c} \cdot \frac{\rho_w}{\rho_c} \cdot c_w \tag{2.2}$$

where ρ_c and ρ_w are the mass density of cartilage and water, and c_c and c_w are the sound velocities in cartilage and water, respectively. In this study, values of ρ_c = 1080 kg/m^3 [7], ρ_w = 1000 kg/m^3, and c_w = 1500 m/s [6] were used.

2.2.5 Calculation of cartilage thickness

Cartilage thickness was calculated by multiplying interval time and sound velocity in the cartilage as follows:

$$H = c \cdot \frac{t_2 - t_1}{2} \tag{2.3}$$

where *H* and *c* are the cartilage thickness and sound velocity, respectively. Constant sound velocity (1600 m/s) [3] and calculated sound velocity were used as *c*.

2.2.6 Needle-probe measurement

The reference thickness of the cartilage samples was measured using the needle method [8], which is shown in Figure 2.3. The specimen was placed on a holder and a sharp needle was pushed vertically into the cartilage at a constant displacement rate. A load cell detected the load signal. The load varied greatly when the needle made contact with the articular surface and cartilage-holder interface, and the displacement distance indicated thickness of the specimen.

2.2.7 Calculation of the relative error of cartilage thickness

The relative error of the ultrasonic measurement of cartilage thickness (measurement error) was determined according to the following equation:

$$e = \frac{H_U - H_N}{H_N} \cdot 100 \qquad (2.4)$$

where e is the relative error, and H_U and H_N are the cartilage thickness from the ultrasound and needle methods, respectively.

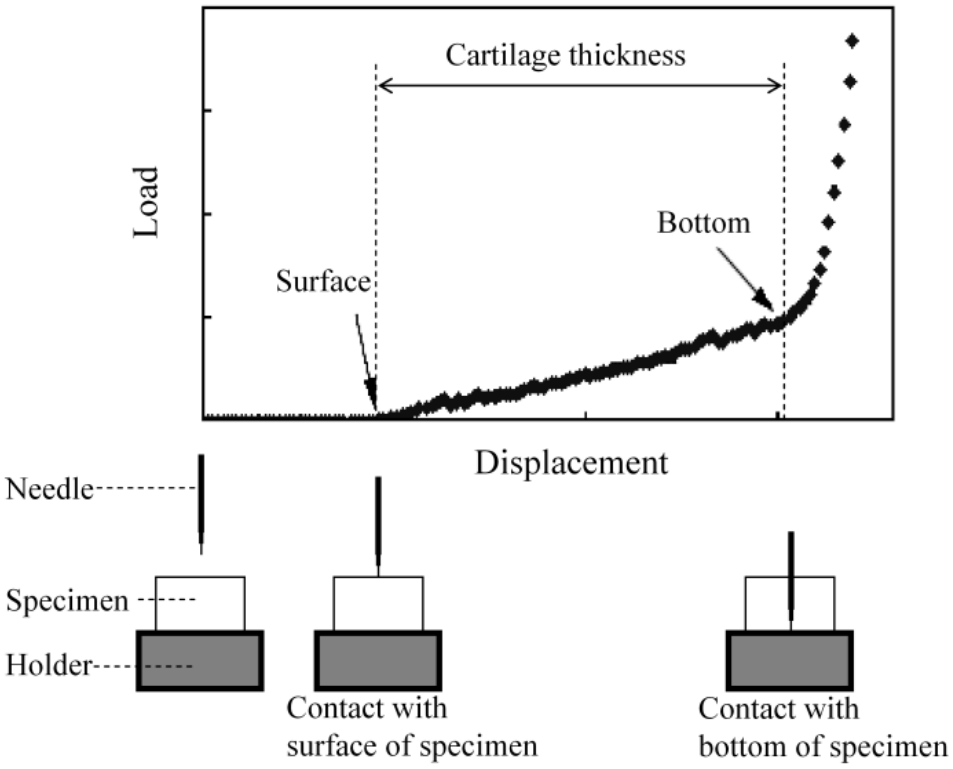

Figure 2.3 Displacement and load signals for the determination of cartilage thickness during a needle test.

2.2.8 Histological observation and biochemical examination

Each cartilage sample was divided into two after the ultrasonic evaluations; one part was used for histological analysis and the other for biochemical analysis. Histological samples were fixed in 10% formalin, decalcified in ethylenediaminetetraacetic acid, and embedded in paraffin. Sagittal sections (5 μm thick) were prepared from the center of the samples and stained with Safranin O. Cartilage samples for biochemical examination were lyophilized overnight after measurement of wet weight. Dry weight was then measured, and water content of the cartilage (as a percentage) was determined according to the following equation: (wet weight–dry weight)/wet weight×100. Samples were then digested by adding 500 μl of 2.5% (w/v) actinase E solution prepared in 100 mM Tris-HCl buffer (pH 8.0), followed by incubation at 55°C for 16 h. Following digestion, samples were boiled for 10 min to inactivate the enzyme, and centrifuged at 10000 g for 15 min to obtain a clear supernatant free of insoluble materials. The amounts of chondroitin 4-sulfate, chondroitin 6-sulfate, and dermatan sulfate were evaluated to quantify proteoglycan content using high-performance liquid chromatography [9]. The amounts of unsaturated tetra- and hexasaccharide of hyaluronic acid were evaluated to quantify hyaluronic acid content [10]. Hydroxyproline content was evaluated to quantify collagen content [11].

2.2.9 Statistical analysis

The Student's t-test was used to determine the effects of enzyme treatment on reflectance ratio, sound velocity, and measurement error. Statistical significance was set at $P<0.05$.

2.3 Result

Figure 2.4 shows the reflectance ratio decreasing exponentially with the enzyme treatment period. The calculated sound velocities in articular cartilage showed the same tendency as the reflectance ratio with significant differences between the 0 h, 4 h, and 9 h groups, as shown in Figure 2.5. The relative errors of thickness measurements using constant sound velocity were -1 (SD 3)% for the 0 h group, 4 (SD 4)% for the 4 h group, and 8 (SD 4)% for the 9 h group; the respective errors using calculated sound velocity were 0 (SD 3)%, -2 (SD 3)%, and -1 (SD 2)%, as shown in Figure 2.6. Significant differences were found using constant sound velocity, whereas the errors using calculated sound velocity showed no significant difference between the groups.

The water contents were 82 (SD 1)% for the 0 h group, 83 (SD 1)% for the 4 h group, and 87 (SD 3)% for the 9 h group; the respective amounts of chondroitin sulfate were 2.5 (SD 0.2)%, 1.9 (SD 0.2)%, and 1.7 (SD 0.2)%, and those of hydroxyproline were 1.2 (SD 0.1)%, 1.3 (SD 0.1)%, and 1.3 (SD 0.2)% (Figures 2.7-2.9). Representative sections of collagenase-digested cartilage stained with Safranin O are shown in Figure 2.10. Homogeneity of Safranin O staining was increased with treatment time and the surface layer to a depth of 200 and 500 μm was not stained with Safranin O after 4 and 9 h, respectively.

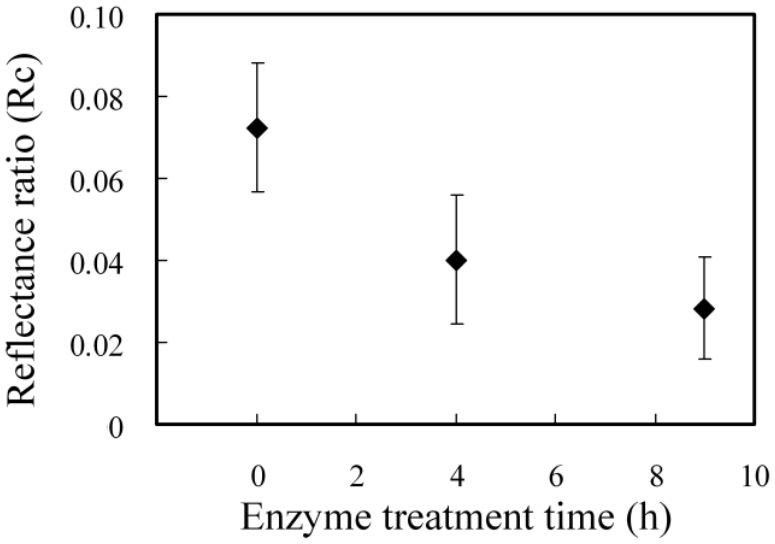

Figure 2.4 Changes in reflectance ratio of an ultrasound echo before (0 h), after 4 hours (4 h), and after 9 hours (9 h) of collagenase digestion. Mean values (SD) are shown for the 0 h (n=10), 4 h (n=10), and 9 h (n=10) groups.

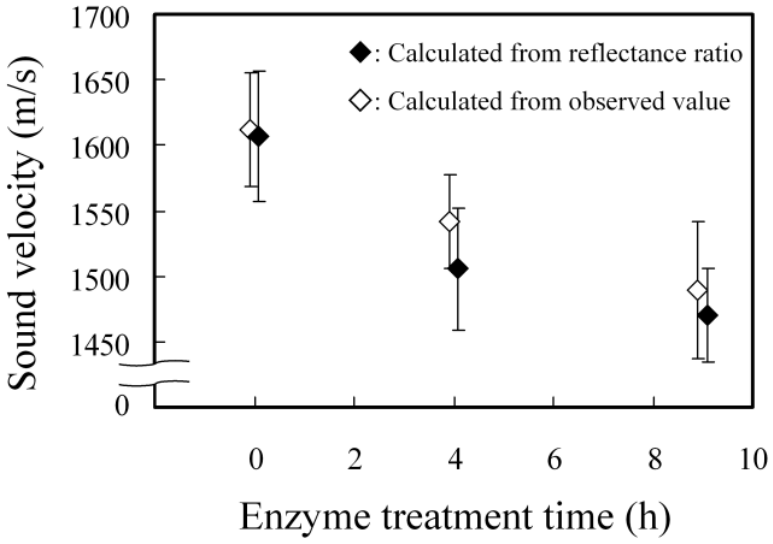

Figure 2.5 Changes in sound velocity calculated from equation (2) and from cartilage thickness measured with needle method and echo interval time before (0 h), after 4 hours (4 h), and after 9 hours (9 h) of collagenase digestion. Mean values (SD) are shown for the 0 h (n=10), 4 h (n=10), and 9 h (n=10) groups.

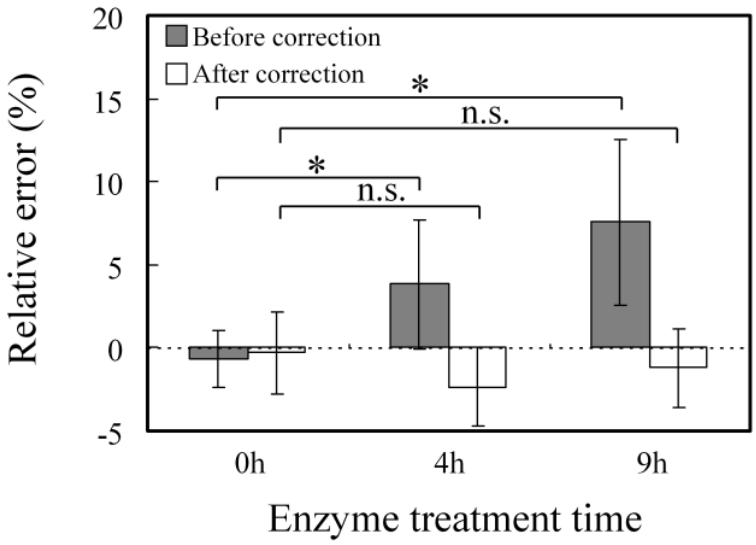

Figure 2.6 Changes in error of thickness measurement before/after correction Mean values (SD) are shown for the 0 h (n=10), 4 h (n=10), and 9 h (n=10) groups. *Significant difference by Student's t-test ($P<0.05$).

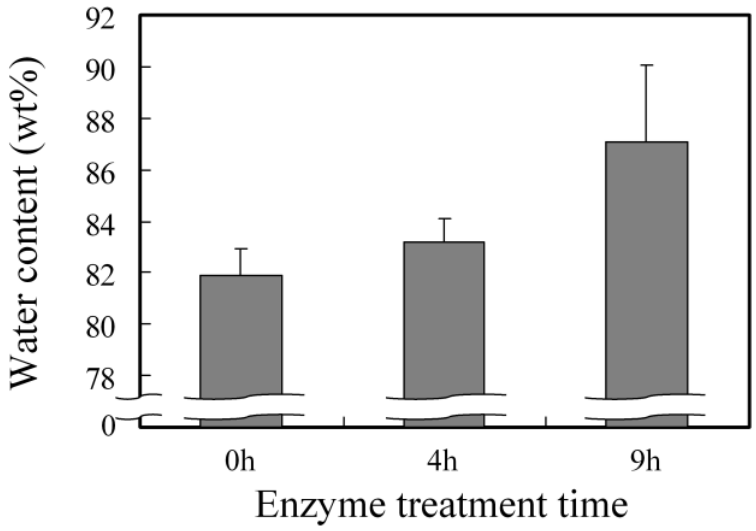

Figure 2.7 Changes in water content in collagenase-digested articular cartilage before (0 h), after 4 hours (4 h), and after 9 hours (9 h) of collagenase digestion. Mean values (SD) are shown for the 0 h (n=10), 4 h (n=10),

and 9 h (n=10) groups.

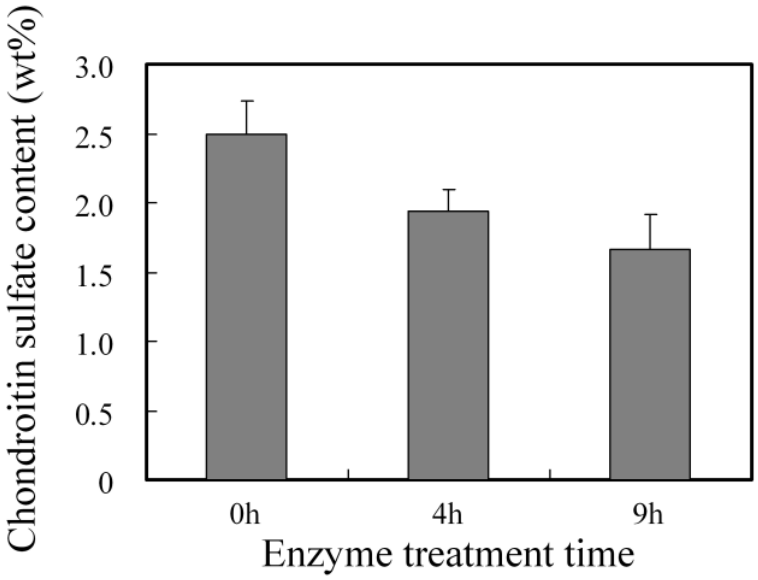

Figure 2.8 Changes in chondroitin sulfate content in collagenase-digested articular cartilage before (0 h), after 4 hours (4 h), and after 9 hours (9 h) of collagenase digestion. Mean values (SD) are shown for the 0 h (n=10), 4 h (n=10), and 9 h (n=10) groups.

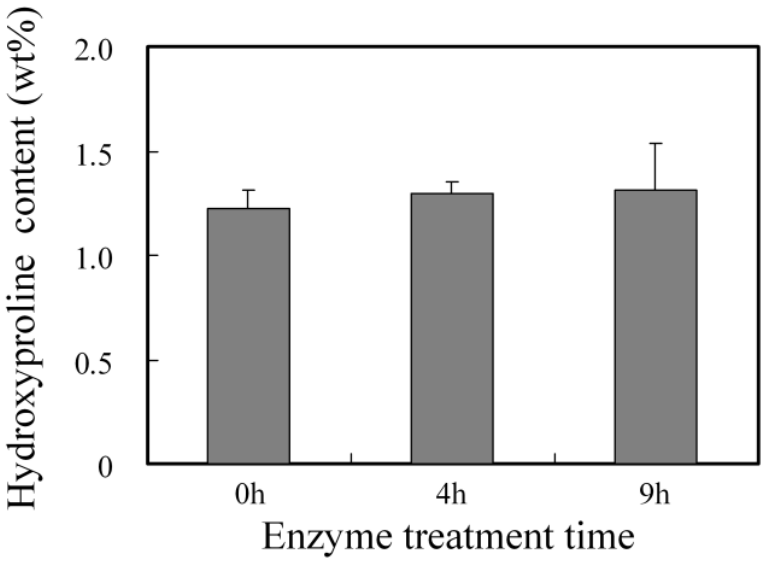

Figure 2.9 Changes in hydroxyproline content in collagenase-digested articular cartilage before (0 h), after 4 hours (4 h), and after 9 hours (9 h) of collagenase digestion. Mean values (SD) are shown for the 0 h (n=10), 4 h (n=10), and 9 h (n=10) groups.

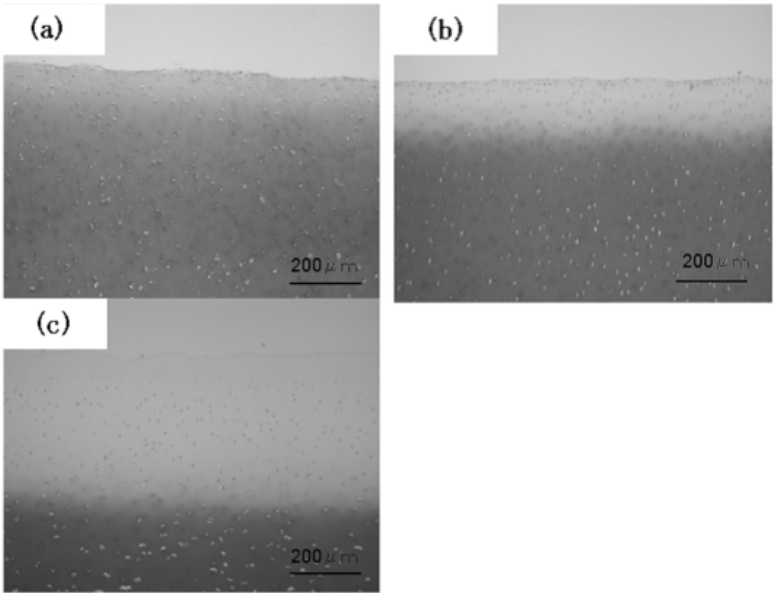

Figure 2.10 Photomicrographs of pig articular cartilage before (a), after 4 hours (b), and after 9 hours (c) of collagenase digestion (Safranin O stain).

2.4 Discussion

Panula et al. reported that an increase in cartilage thickness occurred before macroscopic changes during early OA [12]. Although the accurate value of the increase is not clear, accurate thickness measurement might detect the early stage of OA. Yao and Seedhom indicated that the current ultrasound technique was not sufficiently accurate for measuring cartilage thickness in situ, because change in sound velocity was not considered in the calculation [5]. Myers et al. measured sound velocity in human femoral cartilage using ultrasound and histological measurement, and reported the velocity to be 1658 (SD 185) m/s for normal cartilage and 1581 (SD 148) m/s for OA cartilage [13]. These reports suggest a 10% order of error range of ultrasound thickness measurement for OA cartilage. In the present study, sound velocity in articular cartilage was calculated using echo reflectance from the surface (Rc) and equation (2.2) assuming that the cartilage is homogeneous. The validity of this method was evaluated using collagenase-treated osteochondral plugs, and the treatment-dependent error was reduced from 7% to 2% in absolute value. The applicability of this method for the clinical measurement of cartilage thickness is discussed below.

Firstly, the present calculation still has a systematic error caused by adopting a constant mass density which is difficult to measure directly. The relationship between mass density and water content is shown as follows:

$$\frac{\rho_w V_w}{W_w} = \frac{\rho_p (100 - V_w)}{100 - W_w} \tag{2.5}$$

$$\rho_c = \rho_w V_w + \rho_p (100 - V_w) \tag{2.6}$$

where ρ_c is the mass density of cartilage, W_w is the water content by weight, V_w is the

water content by volume, ρ_w is the mass density of water (ρ_w=1000 kg/m^3), and ρ_p is the mass density of the solid matrix of cartilage (ρ_p=1470 kg/m^3) [14]; the water content increased from 82% to 87%. The mass density of cartilage decreased from 1080 to 1060 kg/m^3 in the present study. As the decrease in mass density increases sound velocity by 2% in equation (2.2), it is suggested that the present method may still have a systematic error of -2% caused by the constant mass density.

Secondly, the effect of the layer structure of cartilage should also be considered. In articular cartilage, the orientation of collagen fibers is different for the superficial tangential zone (parallel to the cartilage surface) compared with the intermediate (random) and deep (perpendicular) zones. Patil et al. reported that sound velocity is higher in the deep zone than in the superficial zone [15]. It suggested that sound velocity calculated using echo from the surface was lower than the average velocity of the whole cartilage. It is possible that the underestimation of velocity causes an underestimation of thickness.

Transection of the meniscus and/or ligaments, and intra-articular injection of a chemical substance such as papain or collagenase are generally performed to induce OA-like changes. In this study, however, collagenase-digested cartilage was used as a model of OA to control the degree of degeneration with high reproducibility. Wilson et al. reported an increase in water content, a decrease in proteoglycan content, and degradation of the collagen network during degeneration of OA cartilage [16]. Additionally, Pritzker et al. reported cationic stain matrix depletion (Safranin O or toluidine blue) which progresses from the surface to the deep layers [17]. As shown in Figures 2.7-10, the same changes were observed in this study using collagenase-treated cartilage. However, additional studies using OA cartilage is required for more precise

evaluation.

It is possible that reflection waveform changes shape with deformation of cartilage surface during OA progression. However, since there are many factors in cartilage surface like surface hydration layer, it is difficult to discuss using simple model. The changes in cartilage surface during OA progression and effect of the changes on reflection waveform are currently under investigation.

In summary, the validity of the correction method for ultrasound measurement of cartilage thickness was evaluated using collagenase-treated osteochondral plugs, where sound velocity in articular cartilage was calculated from reflectance ratios. The collagenase treatment-dependent error was reduced from 7% to 2% in absolute value, which suggests the applicability of the correction method for ultrasound measurement. Studies of several factors such as the difference in surface and layer structure between the enzyme-treated model and degenerated cartilage are recommended for more precise evaluation.

2.5 Reference

[1] Adam, C., Eckstein, F., Milz, S., Schulte, E., Becker, C., Putz, R., The distribution of cartilage thickness in the knee-joints of old-aged individuals measurement by A-mode ultrasound, Clinical Biomechanics, Vol. 13, (1998), pp. 1-10

[2] Hattori K., Mori K., Habata T., Takakura Y., Ikeuch K., Measurement of the mechanical condition of articular cartilage with an ultrasonic probe: quantitative evaluation using wavelet transformation, Clinical Biomechanics, Vol. 18, (2003), pp. 553-557

[3] Laasanen, M.S., Saarakkala, S., Töyräs, J., Hirvonen, J., Rieppo, J., Korhonen, R.K., Jurvelin, J. S., Ultrasound indentation of bovine knee articular cartilage in situ, Journal of Biomechanics, Vol. 36, (2003), pp. 1259-1267

[4] Suh, J.K., Youn, I., Fu, F.H., An in situ calibration of an ultrasound transducer: a potential application for an ultrasonic indentation test of articular cartilage, Journal of. Biomechanics, Vol. 34, (2001), pp. 1347-1353

[5] Yao, J.Q., Seedhom, B.B., Ultrasonic measurement of the thickness of human articular cartilage in situ, Rheumatology (Oxford) Vol. 38, (1999), pp. 1269-1271

[6] National Astronomical Observatory ed., Chronological Scientific Tables. Maruzen Co., Ltd., Japan, (1999)

[7] Shapiro, E.M., Borthakur, A., Kaufman, J.H., Leigh, J.S., Reddy, R., Water distribution patterns inside bovine articular cartilage as visualized by 1H magnetic resonance imaging, Osteoarthritis and Cartilage, Vol. 9, (2001), pp. 533-538

[8] Jurvelin, J.S., Rasanen, T., Kolmonen, P., Lyyra, T., Comparison of optical, needle probe and ultrasonic techniques for the measurement of articular cartilage thickness, Journal of Biomechanics, Vol. 28, (1995), pp. 231-235

[9] Shinmei, M., Miyauchi, S., Machida, A., Miyazaki, K., Quantification of chondroitin 4-sulfate and chondroitin 6-sulfate in pathologic joint fluid, Arthritis & Rheumatism, Vol. 35, (1992), pp. 1304-1308

[10] Takazono I., Tanaka Y., Quantitative analysis of hyaluronic acid by high-performance liquid chromatography of streptomyces hyaluronidase digests, Journal of Chromatograpy, Vol. 84, (1984), pp. 167-176

[11] Woessner, J., The determination of hydroxyproline in tissue and protein samples containing small proportions of this imino acid, Archives of Biochemistry and Biophysics, Vol. 93, (1961), pp. 440-447

[12] Panula, H.E, Hyttinen, M.M, Arokoski, J.P.A, et al., Articular cartilage superficial zone collagen birefringence reduced and cartilage thickness increased before surface fibrillation in experimental osteoarthritis, Annals of the Rheumatic Diseases, Vol. 57, (1998), pp. 237-245.

[13] Myers, S.L., Dines, K., Brandt, D.A., Brandt, K.D., Albrecht, M.E., Experimental assessment by high frequency ultrasound of articular cartilage thickness and osteoarthritic changes, Journal of Rheumatology., Vol. 22, (1995), pp. 109-116

[14] Basser, P.J., Schneiderman, R., Bank, R.A., Wachtel, E., Maroudas, A., Mechanical properties of the collagen network in human articular cartilage as measured by osmotic stress technique, Archives of Biochemistry and Biophysics, Vol. 351, (1998), pp. 207-219

[15] Patil, S.G., Zheng, Y.P., Wu, J.Y., Shi, J., Measurement of depth-dependence and anisotropy of ultrasound speed of bovine articular cartilage in vitro, Ultrasound in Medicine and Biology, Vol. 30, (2004), pp. 953-963

[16] Wilson, W., Van Donkelaar, C.C., Van Rietbergen R., Huiskes, R., The role of computational models in the search for the mechanical behavior and damage mechanisms of articular cartilage, Medical Engineering & Physics, Vol. 27, (2005), pp. 810-826

[17] Pritzker, K P.H., Gay, S., Jimenez, S.A., Ostergaard, K., Pelletier, J.P., Revell, P.A., Salter, D., Van den Berg, W.B., Osteoarthritis cartilage histopathology: grading and staging, Osteoarthritis and Cartilage, Vol. 14, (2006), pp. 13-29

Chapter 3

Measurement of Probe Angle for Ultrasound Evaluation of Articular Cartilage using “Rise-to-Peak time”

3.1 Introduction

Ultrasound evaluation is capable of measuring cartilage thickness and degeneration by analyzing the amplitude of the echo from the cartilage surface [1-3]. However, the echo amplitude changes not only based on the cartilage condition but also on the angle of the ultrasound probe [4]. Therefore the measurer has to make sure the probe is perpendicular to the cartilage surface for accurate measurement. However, there is no reference index of probe angle other than echo amplitude in an endoscopic measurement. This causes measurement error and prolonged measurement time during clinical measurement. Mori et al proposed a measurement support device using robot arm [5]. The automatic scanning of all angles provides accurate measurement. However, the method needs additional equipment.

The aim of this paper is to propose “Rise-to-Peak time” as an index of probe angle. As a first step in evaluating its effectiveness, change in the index associated with probe angle was measured using several reflection surfaces including that of articular cartilage.

3.2 Material and method

3.2.1 Ultrasound measurement

Figure 3.1 shows the ultrasound evaluation system for articular cartilage. The system consisted of a personal computer, a digital oscilloscope, a pulsar/receiver, and a transducer (the ultrasonic probe) (XMS-310, Panametrics Japan Co., Ltd., Tokyo, Japan). The transducer emits a plane wave with a central frequency of 10 MHz, and receives the reflected echo. Articular cartilage plugs with diameters of 8 mm were excised from the patellar surface of porcine knee joints and the specimen was fixed on a stage in water. The perpendicularity between the transducer and the surface of the specimen was ensured by cautious alignment of the stage angle to obtain the maximum echo amplitude. Then the stage angle was changed from 0 degrees up to 5.0 degrees at increments of 0.5 degrees, and the echo amplitude and the "Rise-to-Peak time" were measured from the echo waveforms. Copper and rubber specimens with respective acoustic impedances of 45×10^6 and 2.6×10^6 [Ns/m^3] (calculated from the reflectance ratio) were also measured as references.

3.2.2 Definition of "Rise-to-Peak time"

Figure 3.2 shows a typical ultrasonic echo waveform from the surface of the specimen. The "Rise-to-Peak time" is defined as the time interval between the rise of the first peak (50% amplitude of the first peak) and the first positive peak following the minimum peak of the echo.

3.2.3 Numerical calculation of the "Rise-to-Peak time"

Figure 3.3 shows a simple explanation and the following equations provide a simple method for estimating changes in waveform due to probe angle under the assumption that the angle is small and that the distance between the ultrasound probe and the reflection surface is short (i.e. most of reflected ultrasound wave arrives at the probe). In the two-dimensional model, a is the diameter of the probe, θ is the angle between the ultrasound probe and the reflection surface, and x is the distance from the first point at which the ultrasound wave arrives.

An incident wave per unit area of the probe surface is expressed as

$$f(t) = \frac{1}{a} P(t, 0) \tag{3.1}$$

where $f(t)$ is waveform per unit area and $P(t, 0)$ is the waveform measured at $\theta = 0$.

The delay time for wave arrival at x is expressed as

$$d(x, \theta) = \frac{x \sin 2\theta}{v} \tag{3.2}$$

where $d(x,\theta)$ is the delay time at x, and v is the speed of sound in water.

The measured waveform at angle θ is given by

$$\begin{aligned} P(t, \theta) &= \int_0^a f\left(t - \frac{x \sin 2\theta}{v}\right) dx \\ &= \frac{v}{\sin 2\theta} \left\{ F(t) - F\left(t - \frac{a \sin 2\theta}{v} \right) \right\} \end{aligned} \tag{3.3}$$

where $F(t)$ is the time integral of $f(t)$.

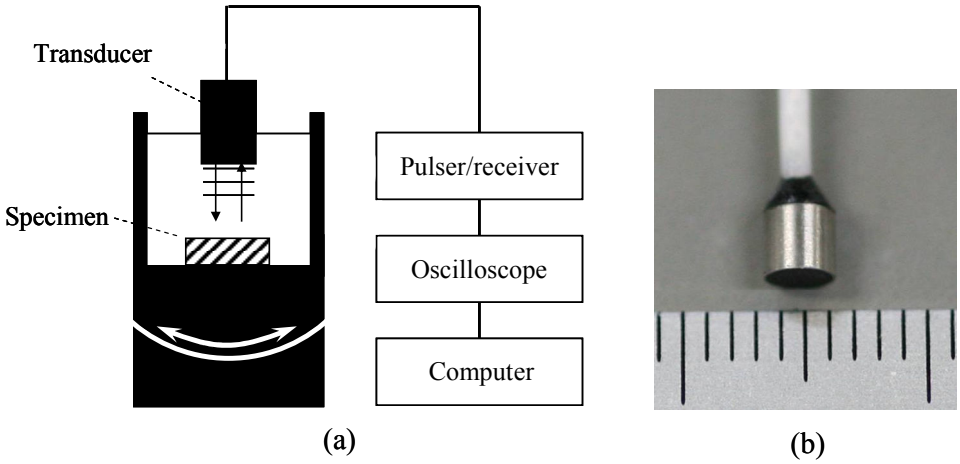

Figure 3.1 (a) Schematic drawing of the ultrasound measurement system. A small transducer was fixed over the measurement device. The measurement was performed in water at room temperature and the A-mode echogram was measured. (b) Ultrasound transducer (diameter: 2mm, frequency: 10MHz).

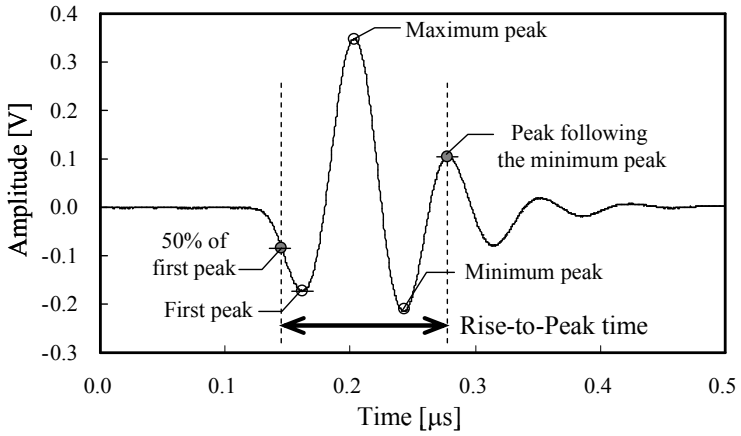

Figure 3.2 Typical pulse waveform of an ultrasound echo. Center frequency: 10 MHz. Sampling frequency: 1 GHz. The "Rise-to-Peak time" is defined as the time interval between the rise of the first peak (50% amplitude of the first peak) and the first positive peak following the minimum peak of the echo.

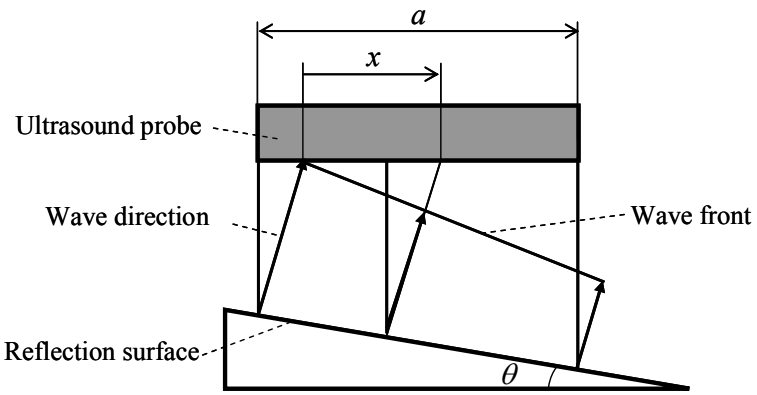

Figure 3.3 Two-dimensional model of a wave incident upon the ultrasound probe. a is the diameter of ultrasound probe, θ is the angle of reflection surface and x is the distance from the first point at which ultrasound wave arrives.

3.2.4 Amplitude correction

The acrylic plates with surface roughness (Rz < 10 μm, Rz = 24, 62 [μm]) were prepared as reflection surface, and the measured echo amplitude was corrected using predetermined relationship between Rise-to-Peak time and reduction rate. The linearly-interpolated data measured using a flat reflection surface was used for the correction.

The measurement error of echo amplitude e was calculated as follows

$$e = \left| \frac{A_0 - A_\theta}{A_0} \right| \cdot 100 \tag{3.4}$$

where A_0 is echo amplitude at 0 degrees without correction. A_θ is echo amplitude at θ degrees. The measurement errors were calculated for the amplitudes before correction and after correction.

3.3 Result

Figure 3.4 shows echo waveforms measured using articular cartilage. The waveforms changed as the angle of the reflection surface changed. However, the waveforms shapes for a specific angle were basically same for each reflection surface. The calculated waveforms shown in Figure 3.5 show the same tendency found in Figure 3.4. Echoes from the articular cartilage surface had lower amplitudes compared with those for the copper and the rubber surfaces, and decreased as the angle of the reflection surface increased as shown in Figure 3.6. However, the reduction rates show same tendency for all reflection surfaces as shown in Figure 3.7. Also, roughing an 80%

decrease was observed for a reflection surface angle of 5.0 degrees.

As shown in Figure 3.8, the “Rise-to-Peak time” increased from 150 ns to 300 ns with an increase in the surface reflection angle from 0 degrees to 5.0 degrees. The “Rise-to-Peak time” increased monotonically with increases in the surface reflection angle despite changes in reflection surface and corresponded well with the calculated values. From these results, the amplitude correction curve of the ultrasound probe used in the present study was composed as shown in Figure 3.9. The “Rise-to-Peak time” also increased from 150 ns to 300 ns with an increase in the surface reflection angle from 0 degrees to 5.0 degrees for the rough surface (Rz < 10 μm, Rz = 24, 62 [μm]) as shown in Figure 3.10. The echoes from the rough surfaces had lower amplitudes compared with those for the flat surface, and decreased as the angle of the reflection surface increased. After the amplitude correction, the decrease of echo amplitude with increase of the angle was suppressed as shown in Figure 3.11. However, the corrected amplitude for higher roughness surface showed higher error value at low angle measurement. Figure 3.12 shows the measurement errors before and after correction. The measurement error was suppressed by the correction at each probe angle in the measurement of Rz < 10 μm and Rz = 24 μm surfaces. However, in the measurement of Rz = 62 μm reflection surface, amplitude correction caused 50% measurement error from 0 degrees.

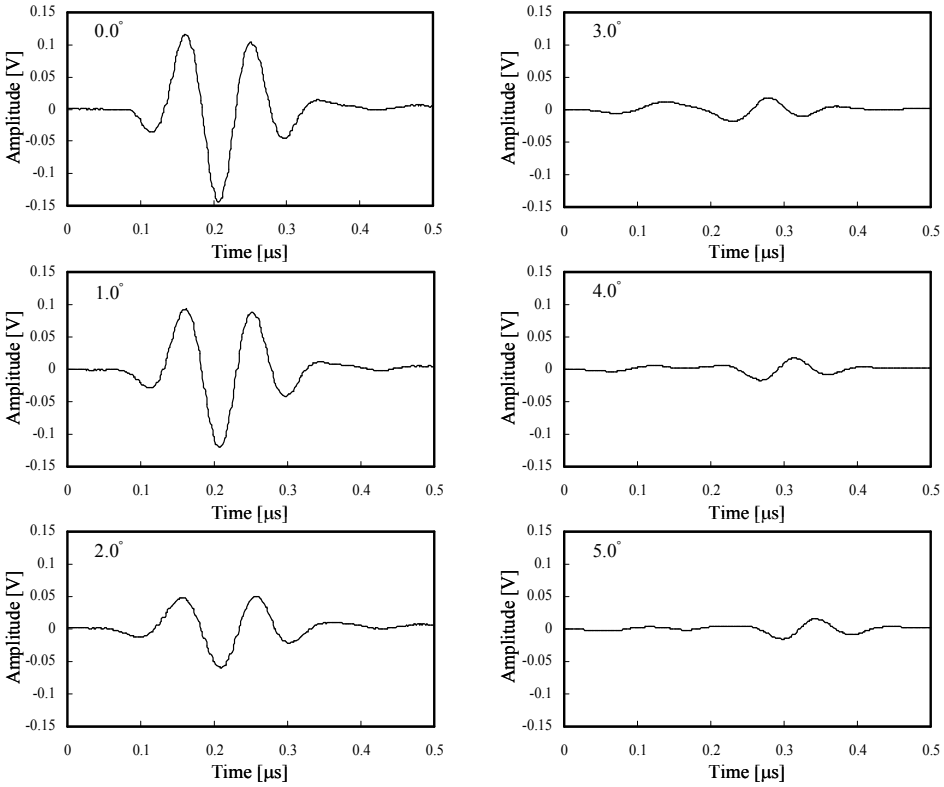

Figure 3.4 Deformation of echo waveforms measured using articular cartilage.

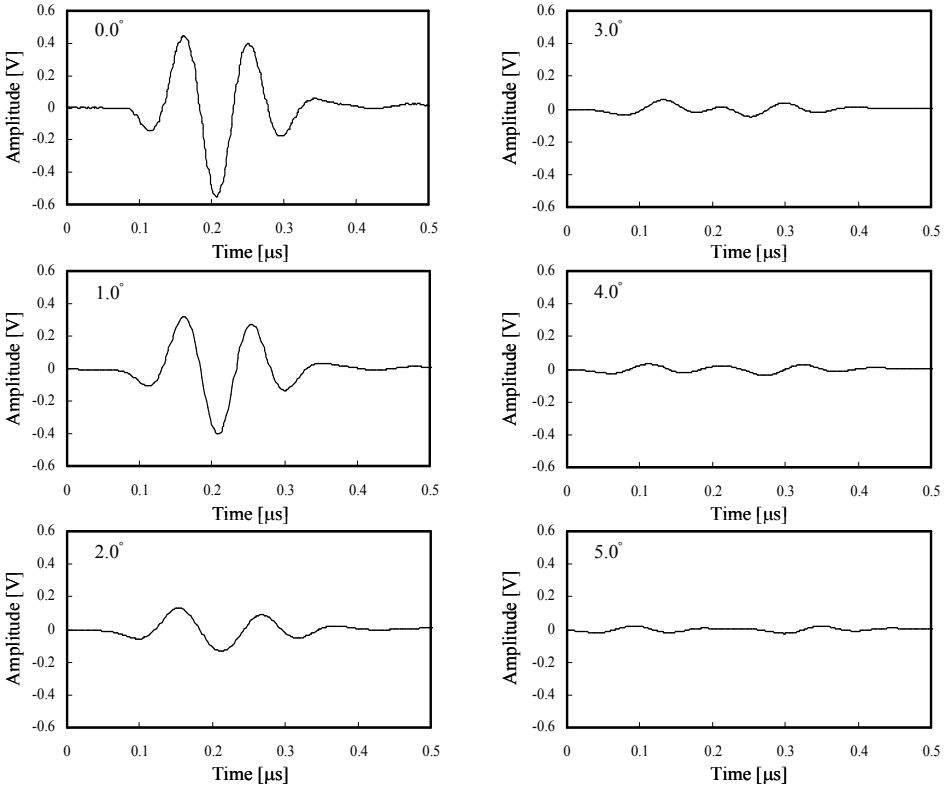

Figure 3.5: Calculated waveforms using equation (3) under the assumption that the reflection surface is flat plate.

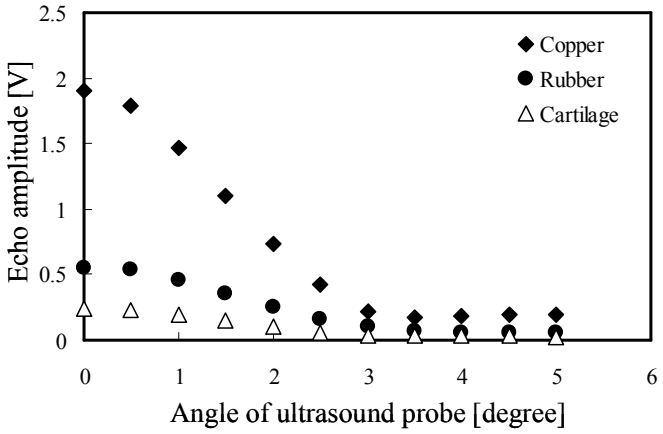

Figure 3.6 Relationship between echo amplitude and probe angle. Copper, rubber and articular cartilage were used as reflection surfaces. Mean values (SD) are shown for 0.0-5.0 degrees.

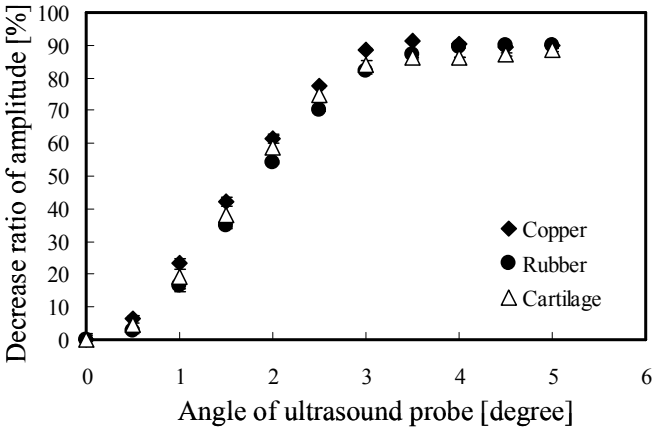

Figure 3.7 Relationship between the decrease ratio of echo amplitude and the probe angle. Mean values (SD) are shown for 0.0-5.0 degrees.

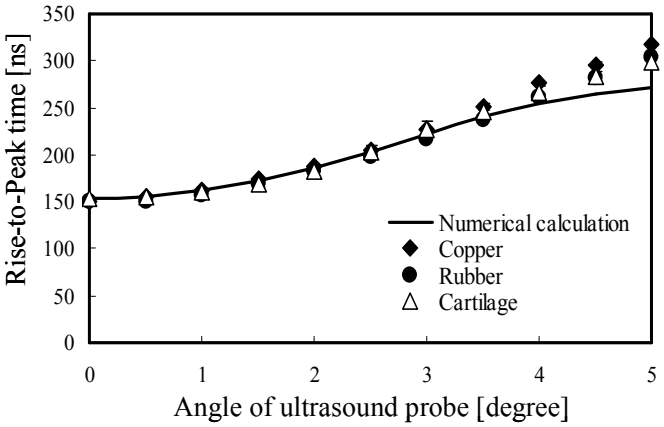

Figure 3.8 Relationship between Rise-to-Peak time and probe angle for the copper, rubber and articular cartilage surfaces. Mean values (SD) are shown for 0.0-5.0 degrees. The solid line shows Rise-to-Peak time of calculated waveforms using equation (3).

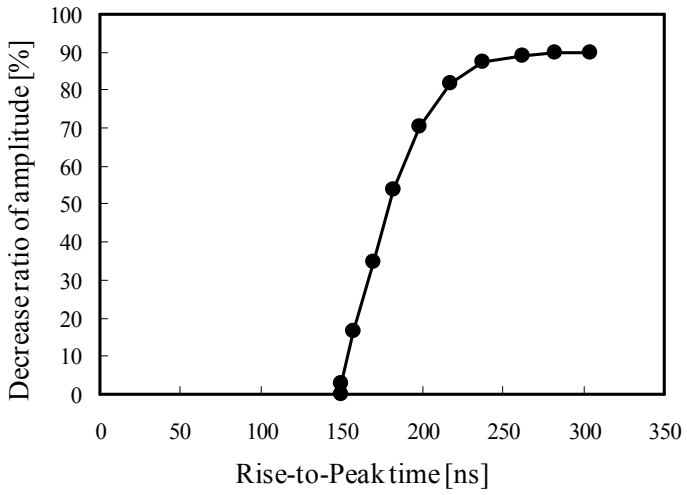

Figure 3.9 The amplitude correction curve of the ultrasound probe used in the present study. The relationship between Rise-to-Peak time and decrease ratio of amplitude measured using flat reflection surface was used to compose the correction curve.

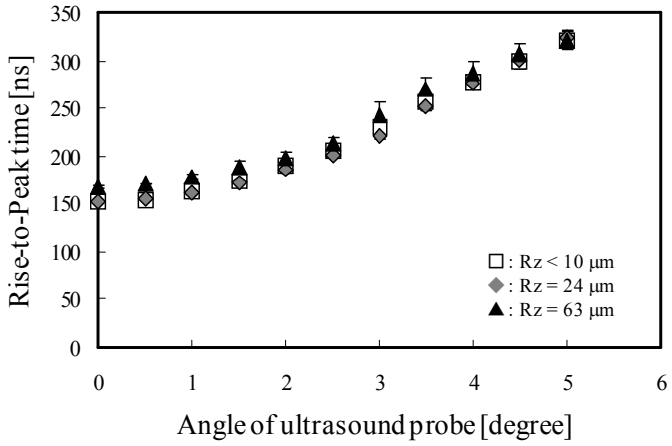

Figure 3.10 Relationship between Rise-to-Peak time and probe angle for the acrylic plates (Rz < 10 μm, Rz = 24 μm, 63 μm). Mean values (SD) are shown for 0.0-5.0 degrees.

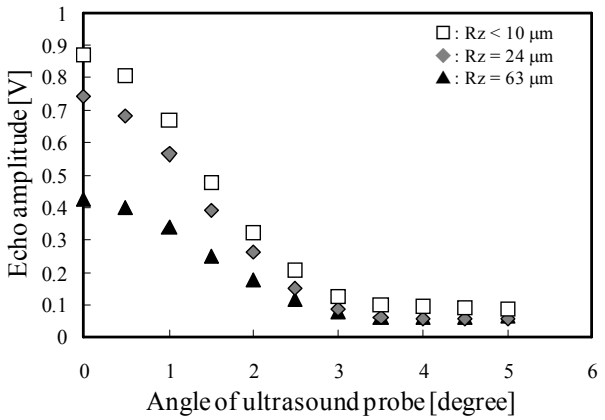

(a): Before calibration

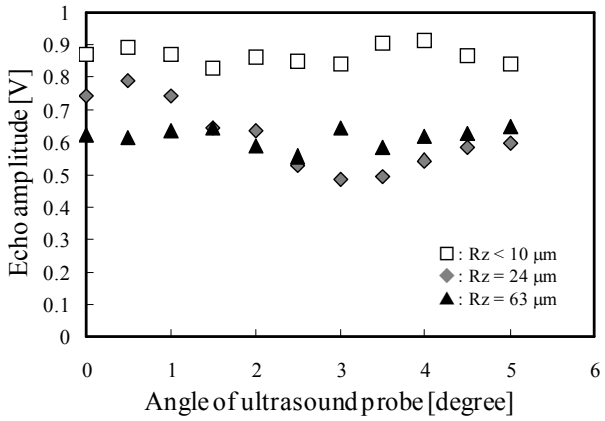

(b): After calibration

Figure 3.11 Relationship between echo amplitude and probe angle. The acrylic plates (Rz < 10 μm, Rz = 24 μm, 63 μm) were used as reflection surfaces. (a): Before calibration. (b): After calibration. Mean values are shown for 0.0-5.0 degrees.

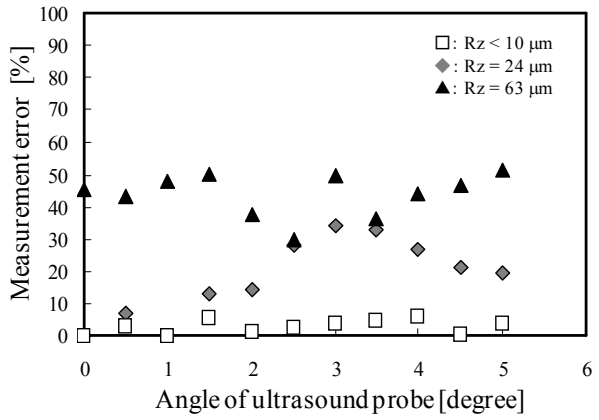

(b): After calibration

1

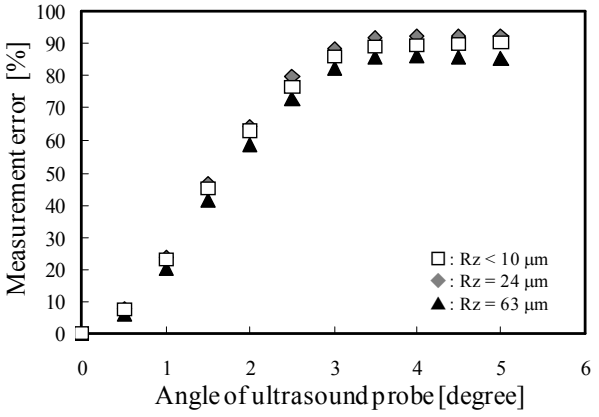

(a): Before calibration

Figure 3.12 Relationship between measurement error and probe angle. The acrylic plates (Rz < 10 μm, Rz = 24 μm, 63 μm) were used as reflection surfaces. (a): Before calibration. (b): After calibration. Mean values are shown for 0.0-5.0 degrees.

3.4 Discussion

This study proposed “Rise-to-Peak time”, which quantifies waveform extension as the index of the angle between the ultrasound probe and the reflection surface, as a method for more accurately measuring slight changes in cartilage condition in early stages of OA. Our simple model calculation shows that “Rise-to-Peak time” increases along with waveform extension caused by increases in probe angle. However, it has been reported that waveform extension also occurs in cases where the reflection surface produces a gradual change in acoustic impedance [6, 7]. As articular cartilage has a layered structure where the orientation and density of collagen fibers changes continuously with depth (Figure 3.13), there is the possibility that the collagen density and orientation produces a gradual change in acoustic impedance [8]. Agemura et al investigated sound velocities from the superficial layer to the deep layer and reported that sound velocity increased with depth from the cartilage surface [9]. Also, the superficial zone is thought to have an outer most hydration layer which has high water content [10].

However, our results showed that the layer structure and hydration layer have very little effect on the reflection and Rise-to-Peak time. The change in velocity in the superficial layer is smaller than the change in the water-cartilage interface [9]. Also, SEM images did not reveal major changes in the density and orientation of collagen fibers from the cartilage surface to the interface of the middle layer [11]. These results suggest that the acoustic impedance changes at a relatively narrow area of the interface between the water and cartilage surface.

Amplitude correction using relationship between the “Rise-to-Peak time” and reduction rate suppressed the probe-angle derived error. However, the correction-derived error

become higher under 2 degrees of probe angle in the measurement of Rz = 62 μm reflection surface. This would be due to neutralizing the effect of the inclined wave incidence caused by the scattering on rough surface.

In early stages of OA, surface roughness of articular cartilage increases from about 5 μm to 100 μm [12], and the change in surface roughness may become one of index for early OA incidence. Our results suggest that the "Rise-to-Peak time" should be exhibit to the measurer as an index of probe learning rather than used for the automatic correction system in order not to erase the effect of surface roughness.

In conclusion, "Rise-to-Peak time" was proposed as an index of probe angle in the clinical ultrasound measurement of articular cartilage. The results showed that the relationship between the "Rise-to-Peak time" and the probe angle for the articular cartilage was similar to those for copper and rubber surfaces. Echo-amplitude correction using the Rise-to-Peak time suppressed the probe-angle derived error, but some correction-derived error could not be negligible under 2 degrees of probe angle in the measurement of Rz = 62 μm reflection surface.

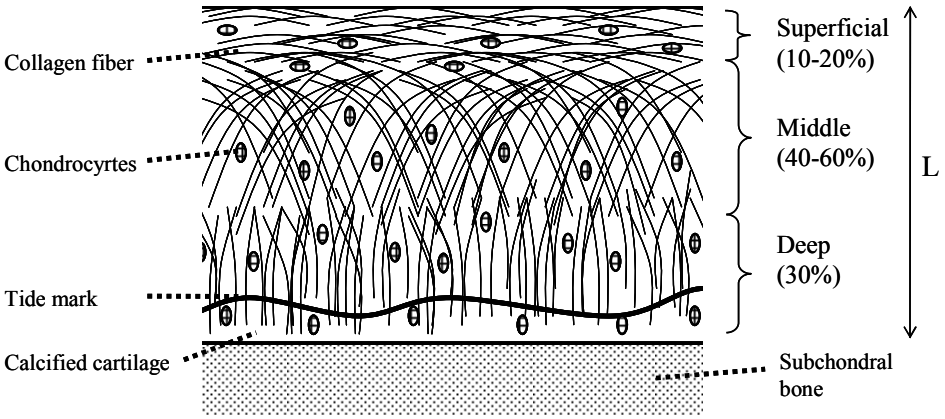

Figure 3.13 Schematic drawing of the layer structure of articular cartilage. In the superficial layer, collagen fibers lie primarily parallel to the cartilage surface. Fibers are randomly oriented in middle layer and perpendicular to the cartilage surface in deep layer. Thickness of the cartilage (L) is about 5 mm for humans.

3.5 Reference

[1] Adam, C., Eckstein, F., Milz, S., Schulte, E., Becker, C., Putz, R., The distribution of cartilage thickness in the knee-joints of old-aged individuals-measurement by A-mode ultrasound, Clinical Biomechanics, Vol. 13, (1998), pp. 1-10

[2] Hattori K., Mori K., Habata T., Takakura Y., Ikeuch K., Measurement of the mechanical condition of articular cartilage with an ultrasonic probe: quantitative evaluation using wavelet transformation, Clinical Biomechanics, Vol. 18, (2003), pp. 553-557

[3] Laasanen, M.S., Saarakkala, S., Töyräs, J., Hirvonen, J., Rieppo, J., Korhonen, R.K., Jurvelin, J.S., Ultrasound indentation of bovine knee articular cartilage in situ, Journal of Biomechanics, Vol. 36, (2003), pp. 1259-1267

[4] Kaleva, E., Saarakkala, S., Jurvelin, J., Virén, T., Töyräs J., Effects of Ultrasound Beam angle and surface roughness on the quantitative ultrasound parameters of articular cartilage, Ultrasound in Medicine & Biology, Vol. 35, (2009), pp. 1344-1351

[5] Yamaguchi University, .Measurement support device for ultrasound arthroscopy, P3689743, 2005-08-31, (in Japanese)

[6] Chivers, R.C., Santosa, F., Numerical considerations for interface reflections in medical ultrasound. Physics in Medicine Biology, Vol. 31, (1986), pp. 819-837

[7] Bruck, H.A., A one-dimensional model for designing functionally graded materials to manage stress waves. International Journal of Solids and Structures, Vol. 37, (2000), pp. 6383-6395

[8] Nieminen, H.J., Töyräs, J., Rieppo, J., Nieminen, M.T., Hirvonen, J., Korhonen, R., Jurvelin, J.S., Real-time ultrasound analysis of articular cartilage degeneration in vitro. Ultrasound in Medicine & Biology, Vol. 28, (2002), pp. 519-525

[9] Agemura, D.H., O'Brien, W.D., Olerud, J.E., Chun, L.E., Eyre, D.E., Ultrasonic propagation properties of articular cartilage at 100 MHz. Journal of the Acoustical Society of America, Vol. 87, (1990), pp. 1786-1791

[10] Nishida K., Inoue H., Murakami T., Immunohistochemical demonstration of fibronection in the most superficial layer of normal rabbit articular cartilage. Annals of the Rheumatic Diseases, Vol. 54, (1995), pp. 995-998

[11] Clark, J.M., The organization of collagen fibrils in the superficial zone of articular cartilage. Journal of Anatomy, Vol. 171, (1990), pp. 117-130

[12] Minns, R.J., Steven, F.S., The collagen fibril organization in human articular cartilage. Journal of Anatomy, Vol. 123, (1977), pp. 437-457

Chapter 4

Effectiveness of Using the “Rise-to-Peak time” Index as a Guide for Ultrasound Evaluation of Articular Cartilage

4.1 Introduction

In a number of recently developed medical fields, such as telesurgery, microsurgery, or arthroscopy [1, 2], the operator is not able to receive direct visual or physical feedback. In these operations, the information is provided to the operator via camera or sensor, and sometimes the information is amplified or converted [3, 4]. However, if the information provided to operator is not intuitive or the information is affected by some disturbance, the operation may become inaccurate or inefficient due to a conflict with the mental model of operator [5]. For example, during ultrasound evaluation of articular cartilage [6-8], accurate evaluation is difficult due to the fact that the probe angle index is affected by disturbances other than probe angle.

Ultrasound can be used to evaluate the elasticity and surface roughness of articular cartilage by analyzing the amplitude of the echo received from the cartilage surface. However, the echo amplitude changes not only with the condition of the cartilage but also with the angle of the ultrasound probe [9]. Therefore the operator must manipulate the ultrasound probe such that the echo amplitude is maximized to make sure that the probe is perpendicular to the cartilage surface. However, if the cartilage surface has some lesions, like the cartilage shown in Figure 4.1, it is possible that this

manipulation using echo amplitude as the index of the probe angle can result in the unconscious avoidance of rough areas due to the reduced amplitude values observed in these rougher regions. This erroneous probe displacement impairs the ability of ultrasound measurement in detecting cartilage degeneration.

We have proposed “Rise-to-Peak time” as a new index of probe angle and have investigated the effectiveness of this index in the automatic amplitude correction [10]. Unlike the echo amplitude index, the “Rise-to-Peak time” is mainly a function of probe angle and is little-affected by the elasticity and surface roughness of reflection surface. Therefore, the echo amplitude index can be corrected using the relationship between the “Rise-to-Peak time” and decrease ratio of echo amplitude. However, previous results showed that automatic amplitude correction using the “Rise-to-Peak time” causes correction-derived errors due to the neutralization of the effect of the surface roughness on echo amplitude [10].

The aim of this study is to evaluate the effectiveness of using the “Rise-to-Peak time” index to the display of the directly inform the operator of the probe angle during ultrasound measurement. The “Acceptance” index was defined to evaluate the superiority of Rise-to-Peak time compared with echo amplitude in decreasing erroneous displacement of the measurement point.

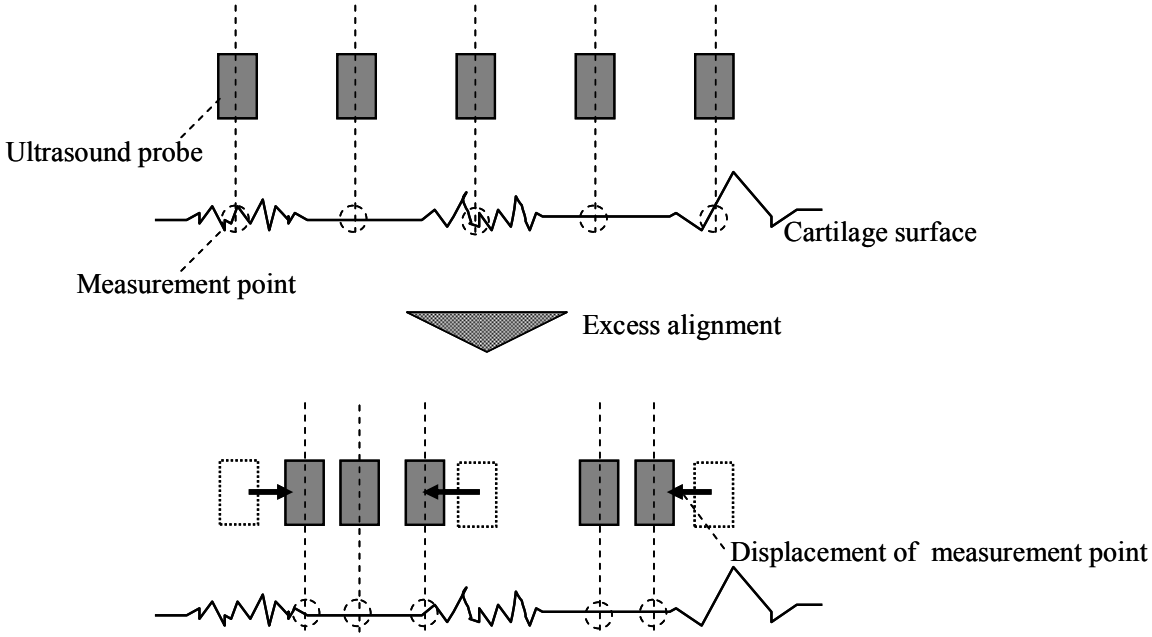

Figure 4.1 The operator manipulates ultrasound probe to make the echo amplitude maximum to make sure the probe is perpendicular to the cartilage surface. In the case of the measurement of cartilage surface that has some lesions, it is possible that measurer unconsciously avoids rough area.

4.2 Material and Method

4.2.1 Ultrasound measurement

Figure 4.2 shows the ultrasound evaluation system used for measuring articular cartilage. The system consisted of a personal computer, a digital oscilloscope, a pulsar/receiver, and a transducer (the ultrasonic probe) (XMS-310, Panametrics Japan Co., Ltd., Tokyo, Japan). The transducer emits and receives the ultrasound wave, while a plane wave with a central frequency of 10 MHz is oscillated from the transducer.

Acrylic plates with uneven surface roughness (flat surface: Rz < 10 μm, middle rough surface: Rz = 24 μm, rough surface: Rz = 62 μm) were prepared as reflection surfaces. The surface roughness was created using sandpaper and measured by a surface roughness measuring instrument (Surfcorder SE1200, Kosaka Laboratory Ltd.).

The specimen was fixed on a stage in water and the perpendicularity between the transducer and the surface of the specimen was ensured by cautious alignment of the stage angle to obtain the maximum echo amplitude. Then the stage angle was changed from 0 degrees up to 5.0 degrees at increments of 0.5 degrees, and the echo amplitude and the “Rise-to-Peak time” were measured from the echo waveforms.

The “Rise-to-Peak time” is defined as the time interval between the rise of the first peak (50% amplitude of the first peak) and the first positive peak following the minimum peak of the echo (Figure 4.3).

4.2.2 Calculation of "Acceptance" value

The "Acceptance" was defined as the normalized difference between the index values at 0 degrees for the middle rough and rough surfaces and the values at 0 to 5 degrees for the flat surface.

$$\text{Acceptance} = \frac{index(0°, Y\mu m) - index(x°, 0\mu m)}{index(0°, 0\mu m) - index(5°, 62\mu m)} \quad (4.1)$$

where *index(X, Y)* is the echo amplitude or Rise-to-Peak time at *X* degrees in the measurement of Rz = *Y* μm reflection surfaces. Acceptance values were calculated from 0 to 5.0 degrees for the middle rough and rough surfaces.

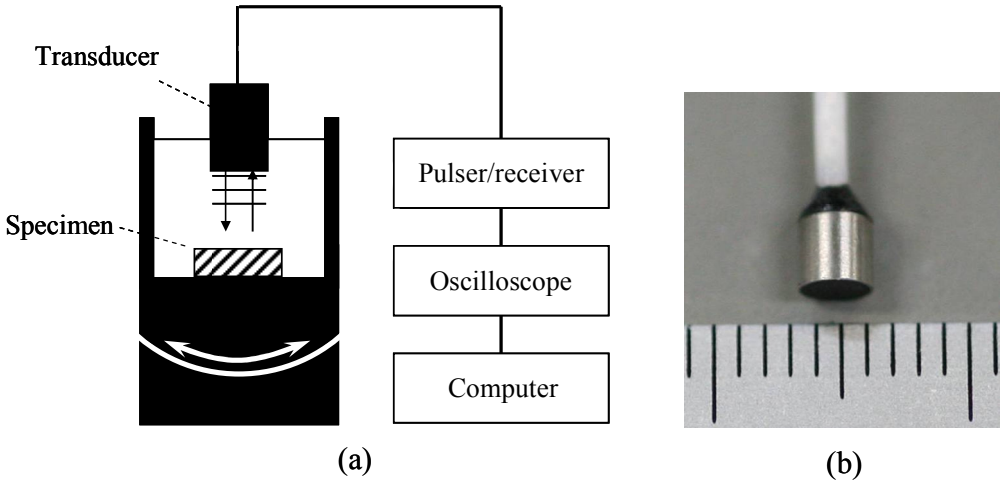

Figure 4.2 (a) Schematic drawing of the ultrasound measurement system. A small transducer was fixed over the measurement device. The measurement was performed in water at room temperature and the A-mode echogram was measured. (b) Ultrasound transducer (diameter: 2mm, frequency: 10MHz).

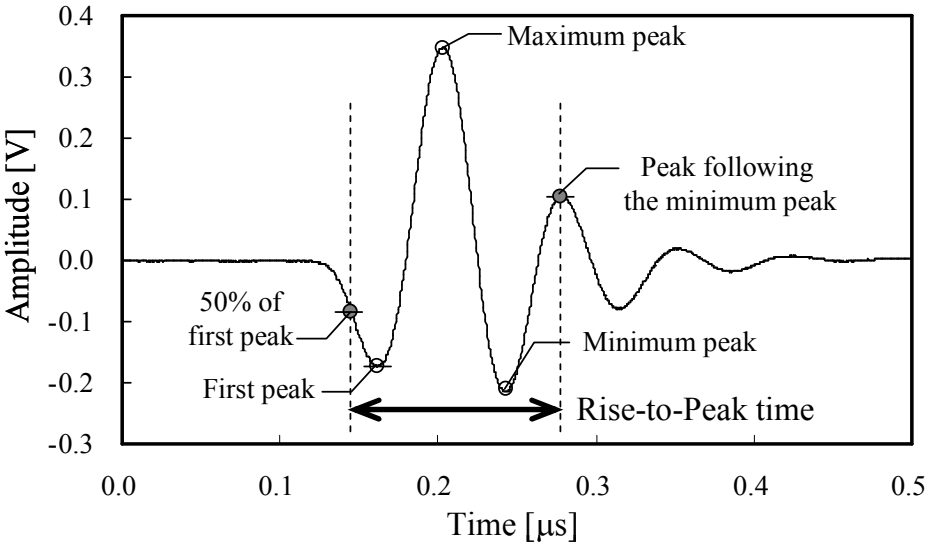

Figure 4.3 Typical pulse waveform of an ultrasound echo. Center frequency: 10 MHz. Sampling frequency: 1 GHz. The "Rise-to-Peak time" is defined as the time interval between the rise of the first peak (50% amplitude of the first peak) and the first positive peak following the minimum peak of the echo.

4.3 Result

Echoes from the middle rough and rough surfaces had lower amplitudes compared with those for the flat surface, and decreased as the angle of the reflection surface increased as shown in Figure 4.4. Roughly an 80% decrease was observed for a reflection surface angle of 3.0 degrees, and minor decrease was observed from 3.0 degrees to 5.0 degrees. As shown in Figure 4.5, the "Rise-to-Peak time" increased from 150 ns to 300 ns with an increase in the surface reflection angle from 0 degrees to 5.0 degrees. The echo from rough surface (Rz = 62 μm) had slightly-high Rise-to-Peak time compared with flat surface.

The calculated "Acceptance" was shown in Figure 4.6. For the calculation of the middle rough surface, the echo amplitude had a negative Acceptance from 0 to 0.5 degrees. Meanwhile, the Rise-to-Peak time did not have any negative Acceptance values. For the high rough surface, the Rise-to-Peak time also had negative values, but the absolute values were small compared with those for echo amplitude.

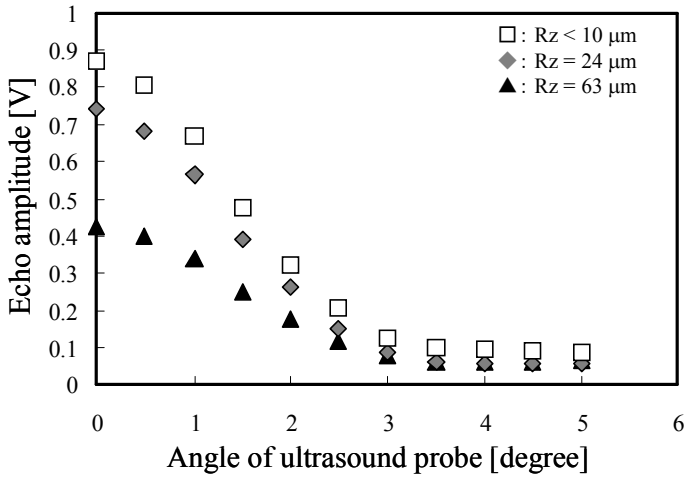

Figure 4.4 Relationship between echo amplitude and probe angle. The acrylic plates (Rz < 10 μm, Rz = 24 μm, 62 μm) were used as reflection surfaces.

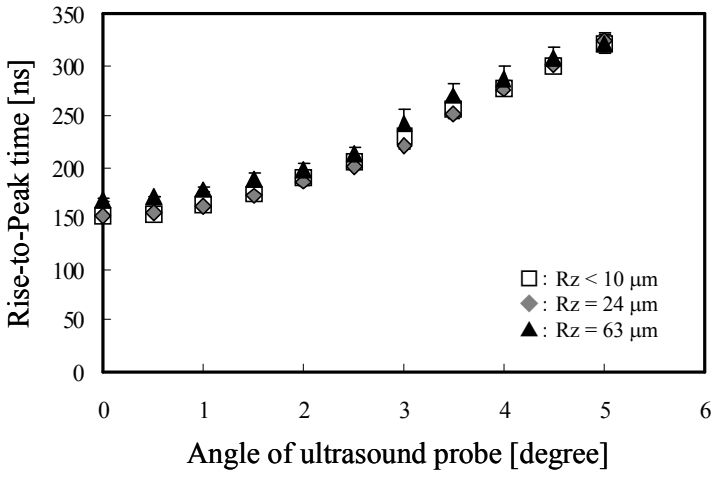

Figure 4.5 Relationship between Rise-to-Peak time and probe angle for the acrylic plates (Rz < 10 μm, Rz = 24 μm, 62 μm). Mean values (SD) are shown for 0.0-5.0 degrees

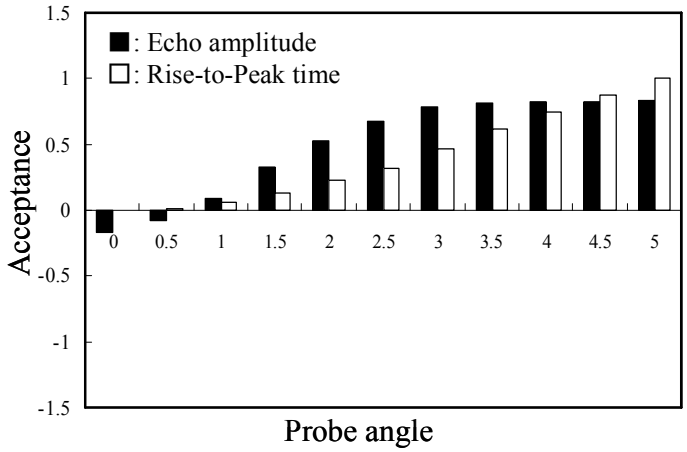

(a): The calculation for middle rough surface (Rz = 24 μm)

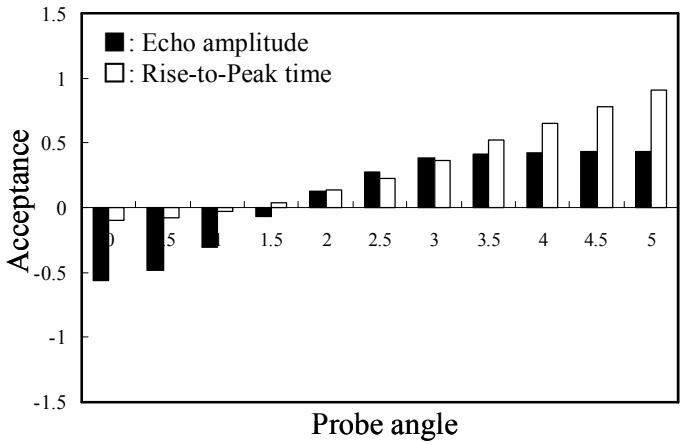

(b): The calculation for rough surface (Rz = 62 μm).

Figure 4.6 The Acceptance of echo amplitude and Rise-to-Peak time calculated from equation (1). (a): The calculation for the middle rough surface (Rz = 24 mm). (b): The calculation for the rough surface (Rz = 62 mm).

4.4 Discussion

The fundamental concept of the "Acceptance" value is defined as the normalized difference between the index values at a standard position and at a deviated position where there are disturbance.

$$\text{Acceptance} = \frac{index(x_0, y_0) - index(x, y)}{\Delta index(X, Y)} \tag{4.2}$$

where $index(x_0,y_0)$ is the index at a standard position (x_0,y_0) , $index(x,y)$ is the index at a deviated position (x,y) with a disturbance:y-y_0, and $\Delta index(X,Y)$ is the maximum range of the index within a specific measurement area (X,Y). The negative "Acceptance" value indicates that the influence of the disturbance:y-y_0 on the index value exceeds that of x-x_0, where the correction operation may be more affected by the change in the disturbance and result in an erroneous position.

The present study shows an example application of the "Acceptance" value using the "Rise-to-Peak time" as the index and surface roughness as the disturbance. Figure 4.7 shows the effects of the probe angle and surface roughness on the echo amplitude and the Rise-to-Peak time. As the echo amplitude changes not only with probe angle but also with surface roughness, the operation to maximize the echo amplitude tends to deviate the measuring position to the smoother surface region. In this study, superiority of the Rise-to-Peak time for the manual measurement was numerically evaluated using the "Acceptance" value.

The probe angle alignment was modeled as shown in Figure 4.8. The operator swings the probe in one direction guided by the angle index. After observing the index pass through an extreme value, the operator moves the probe in the opposite direction.

Figure 4.8(b) shows a conceptual drawing of the time course of the manual measurement operation, where the operator finishes the measurement at the convergence of swing amplitude. However, if there is a disturbance such as change in surface roughness, it is possible that the maximum or minimum value in the sequences exceeds the convergence value. In this case, as it becomes more difficult for the operator to feel the convergence of the index, an increase in both the measurement time and the attendant displacement from the measurement point occur. In this study, this difference between the maximum or minimum value and the convergence value was used as the "Acceptance" for evaluating the effectiveness of the Rise-to-Peak time and the echo amplitude indexes. The negative Acceptance means that the index value has exceeded the convergence value. The large negative Acceptance and the wide angle range where the negative acceptance occurs show an increase in the possibility for increased measurement time and erroneous displacement of the measurement point. As shown in Figure 4.6, the Rise-to-Peak time index did not have a large negative Acceptance compared with that for the echo amplitude index. Also, the angle range within which the Rise-to-Peak had negative Acceptances was small. The results show that using Rise-to-Peak time index is an effective way to decrease both measurement time and erroneous displacement of the measurement point.

Compared to the automatic amplitude correction using Rise-to-Peak time, the measurement supported by displaying the Rise-to-Peak time might require a longer measurement time. Also, compared to the automatic scanning of all angles by robot arm [11], this support method may lack accuracy. However, this support method does not involve correction-derived error and might provide a more intuitive measurement operation without additional equipment. In clinical use, because the operator has to

watch an arthroscopic image, the Rise-to-Peak time is displayed by sound. The design of the relation between the Rise-to-Peak time and pitch or loudness of a sound would be the focus of a near-future study.

In conclusion, the effectiveness of the displaying the “Rise-to-Peak time” to the operator during ultrasound measurement was evaluated. The results showed that displaying the Rise-to-Peak time was the potential to decrease both measurement time and erroneous displacement of the measurement point compared with using echo amplitude as the angle index.

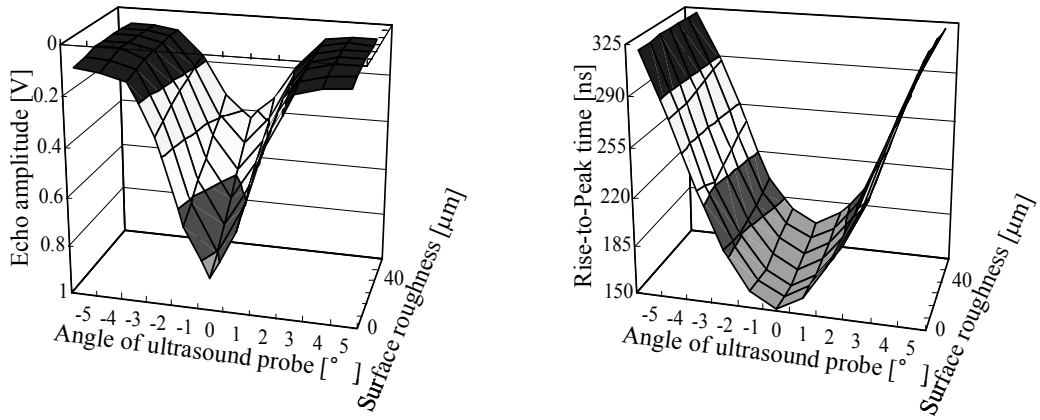

Figure 4.7 The effects of the probe angle and surface roughness on the echo amplitude and the Rise-to-Peak time. (a): Echo amplitude. (b): Rise-to-Peak time.

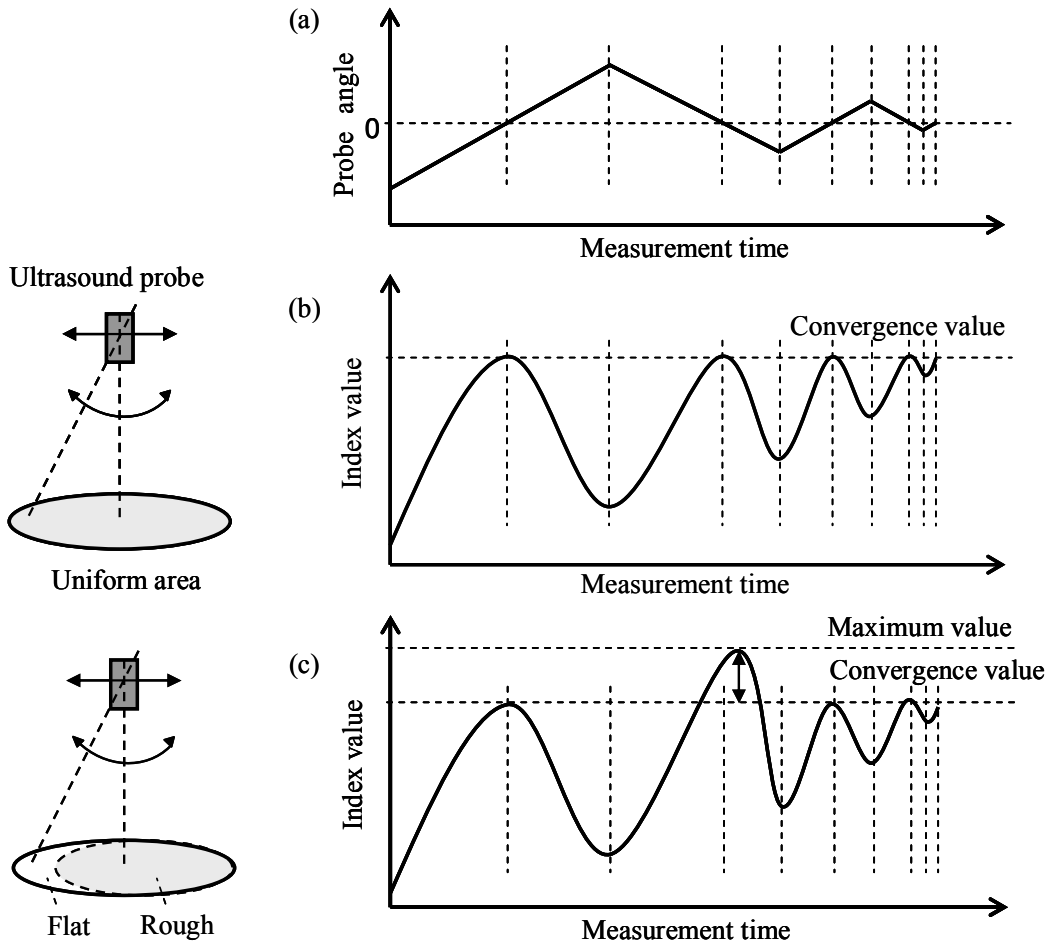

Figure 4.8 The probe angle alignment model. (a): The time course of probe angle. (b): The time course of the index in the measurement of uniform area. (c): The time course of the index in the measurement of the rough surface near the flat surface.

4.5 Reference

[1] Ballantyne, G.H., Robotic surgery, telerobotic surgery, telepresence, and telementoring, Surgical Endoscopy, Vol. 16, (2002), pp. 1389-1402

[2] McGinty, J.B., Burkhart, S.S., Operative arthroscopy, Lippincott Williams & Wilkins, (2003)

[3] Mitsuishi, M., Kobayashi, K., Nagao, T., Hatamura, Y., Sato, T., Kramer, B.,Development of Tele-Operated Micro-Handling/Machining System Based on Information Transformation, Proceedings of the 1993 IEEE/RSJ International Conference on Intelligent Robots and Systems, (1993), pp. 1473-1478

[4] Norman, D.A., The design of every things, New York, NY: Doubleday, (1990)

[5] Wang, S., Ding, J., Yun, J., Li, Q., A robotic system with force feedback for microsurgery, Proceedings of the 2005 IEEE International Conference on Robotics and Automation, (2005), pp. 200–205

[6] Adam, C., Eckstein, F., Milz, S., Schulte, E., Becker, C., Putz, R., The distribution of cartilage thickness in the knee-joints of old-aged individuals-measurement by A-mode ultrasound, Clinical Biomechanics, Vol. 13, (1998), pp. 1–10

[7] Hattori K., Mori K., Habata T., Takakura Y., Ikeuch K., Measurement of the mechanical condition of articular cartilage with an ultrasonic probe: quantitative evaluation using wavelet transformation, Clinical Biomechanics, Vol. 18, (2003), pp. 553–557

[8] Laasanen, M.S., Saarakkala, S., Töyräs, J., Hirvonen, J., Rieppo, J., Korhonen, R.K., Jurvelin, J.S., Ultrasound indentation of bovine knee articular cartilage in situ, Journal of Biomechanics, Vol. 36, (2003), pp. 1259–1267

[9] Kaleva, E., Saarakkala, S., Jurvelin, J., Virén, T., Töyräs J., Effects of Ultrasound Beam angle and surface roughness on the quantitative ultrasound parameters of articular cartilage, Ultrasound in Medicine & Biology, Vol. 35, (2009), pp. 1344–1351

[10] Yamada, K., Oda, K., Tomita, N., Measurement of probe angle for ultrasound evaluation of articular cartilage using “Rise-to-Peak time”, Journal of Biomechanical Science and Engineering, Vol. 5, (2010), pp. 615-624

[11] Yamaguchi University, Measurement support device for ultrasound arthroscopy, P3689743, 2005-08-31, (in Japanese)

Chapter 5

Evaluation of the Effectiveness of the Rise-to-Peak time during an Angle Alignment Task by the User Study

5.1 Introduction

In ultrasound measurement of articular cartilage, measurement error occurs if the ultrasound probe is not perpendicular to the cartilage surface [1]. In clinical ultrasound measurement, echo amplitude can be used as the angle index. However, because echo amplitude is affected by disturbances such as cartilage surface roughness, the use of echo amplitude can result in inaccurate probe angle alignment and the unconscious probe displacement. Recently, Rise-to-Peak time was proposed as the probe angle index. The effectiveness of Rise-to-Peak time was evaluated using the "Acceptance" described earlier, and it was predicted that the display of the Rise-to-Peak time can decrease measurement time and unconscious probe displacement compared with using echo amplitude as the angle index [2].

The aim of this study is to evaluate the effectiveness of Rise-to-Peak time during an angle alignment task by the user study. The stick angle alignment task using a Rise-to-Peak time-type index and an echo amplitude-type index was performed, and the effect of the indexes on the performance of the task was evaluated.

5.2 Material and method

5.2.1 Composition of test system

For the user test, a test system that imitates the operation of the alignment the probe angle in ultrasound evaluation was constructed. Figure 5.1 shows a schematic view of the test system. The system was constructed of a stick with sensors for stick position and angle (PHANTOM Omin, Sensable), a PC display, and a headphone.

5.2.2 Imaginary plane and definition of stick angle and stick position

As shown in Figure 5.2, the imaginary plane was placed under the stick. The stick angle was defined as the relative angle between the normal line of the imaginary plane and the stick axis. Also, the stick position was defined as the poison of the intersection point of the stick axis and the imaginary plane.

5.2.3 Surface roughness parameter

The “surface roughness parameter” is defined by the following equation.

$$R = \begin{cases} \frac{1}{40}x + \frac{1}{2} & (-20 < x < 20) \\ 0 & (x \leq -20) \\ 1 & (x \geq 20) \end{cases} \tag{5.1}$$

Where R is the surface roughness parameter and x is the x-coordinate of the stick position. Figure 5.3 shows a schematic view of the distribution of the surface roughness parameter.

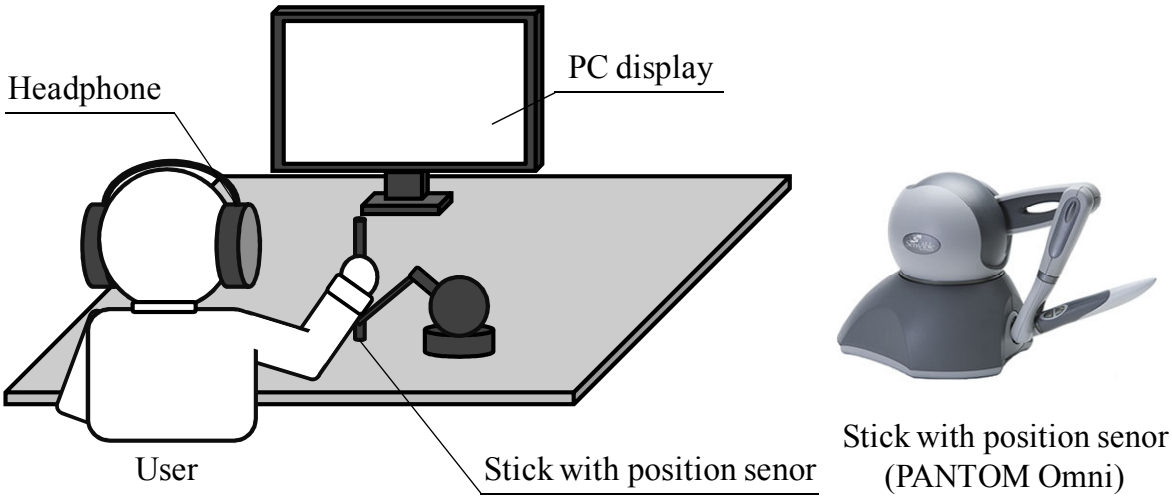

Figure 5.1 The schematic drawing of the user test system. The system was constructed of a stick with sensors for stick position and angle (PHANTOM Omin, Sensable), the PC display, and the headphone.

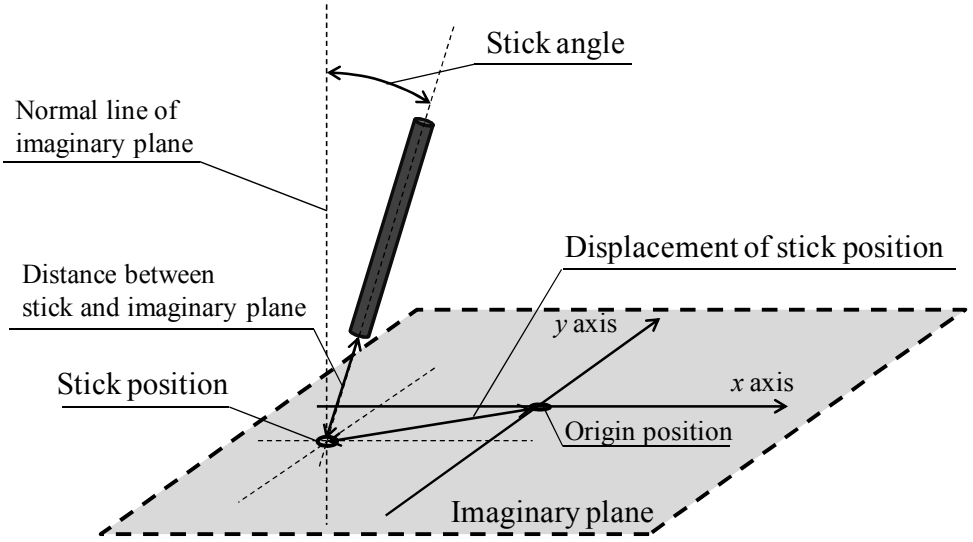

Figure 5.2 The schematic drawing of the imaginary plane. The stick angle is the relative angle between the normal line of the imaginary plane and the stick axis. The stick position is the poison of the intersection point of the stick axis and the imaginary plane. The displacement of the stick is the distance between the origin position and the stick position.

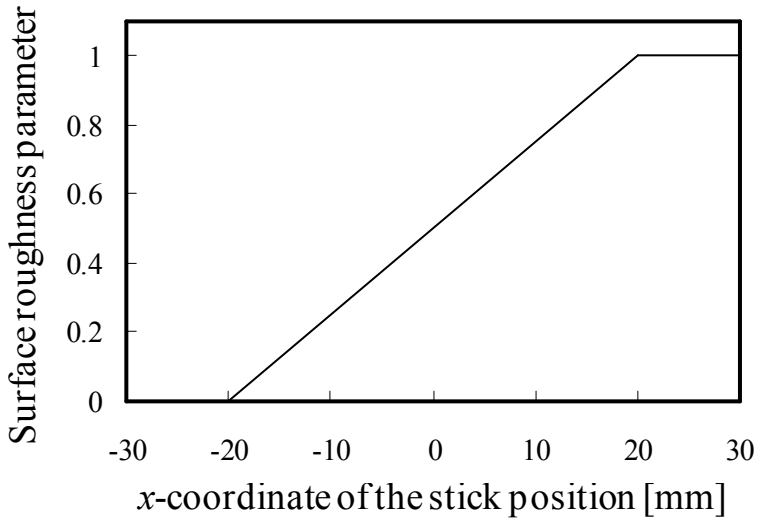

Figure 5.3 The relationship between the surface roughness parameter and the x-coordinate of the stick position.

5.2.4 Indexes of stick angle

Three types of the stick angle index were used in this study. First is the "Ideal" index that changes with only the stick angle. Second is the "Rise-to-Peak time-type" index that changes with the stick angle and with the surface roughness parameter slightly. Third is the "Echo amplitude-type" index that changes with the stick angle and the surface roughness parameter greatly. The values of these indexes are expressed as follows.

$$I_I = 100 \times \frac{\theta}{15} \tag{5.2}$$

$$I_R = 10R + (100 - 10R) \times \frac{\theta}{15} \tag{5.3}$$

$$I_A = 60R + (100 - 60R) \times \frac{\theta}{15} \tag{5.4}$$

where θ is the stick angle, I_I, I_R and I_A are the values of the ideal index, the Rise-to-Peak time-type index, and the Echo amplitude-type index, respectively. Figure 5.4 shows the relationships between the probe angle and the angle indexes.

5.2.5 Presentation of angle index

The angle indexes were presented as auditory feedback using headphone. The change of index was presented as the change of the sound frequency and the sound volume as follows.

$$V = 49 + 36 \times \frac{I}{100} \tag{5.5}$$

$$f = 440 + 440 \times \frac{I}{100} \tag{5.6}$$

where V is the sound volume [dBA], f is the sound frequency [Hz], and I is the values of the index.

5.2.6 Presentation of distance between the stick and the imaginary plane

The distance between the stick head and the intersection point of the stick axis and the imaginary plane was presented as the position of the slide bar on the PC display (Figure 5.5). The position of the slide bar varies with the distance between the stick and the imaginary plane, and becomes the center position when the stick is kept at the right distance (50 mm).

5.2.7 Procedure of user test

The user test of the angle alignment task was performed through following procedure. At first, the user sets the stick potion to the origin position (x = 0, y = 0), while the imaginary plane is displayed on the PC display (Figure 5.5). After this, the user attempts to align the stick perpendicular to the imaginary plane by using the auditory feedback. At the same time, the user aligns the distance between the stick and the imaginary plane by reference to the slide bar on the PC display. The test ends when the user thinks that the stick is perpendicular to the imaginary plane. The operation time, the final stick angle, and the displacement of the stick position from the origin position are also recorded. This procedure was repeated 5 times for each angle index. Nine men in their twenties participated in this user test. Table 5.1 shows the order of the test.

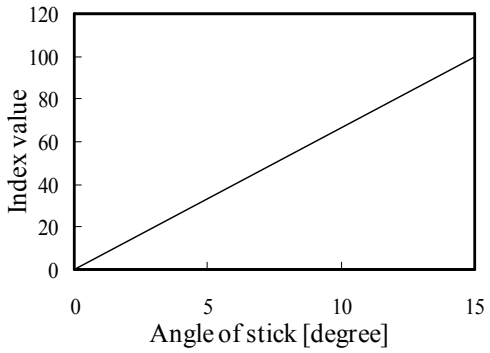

(a) Ideal index

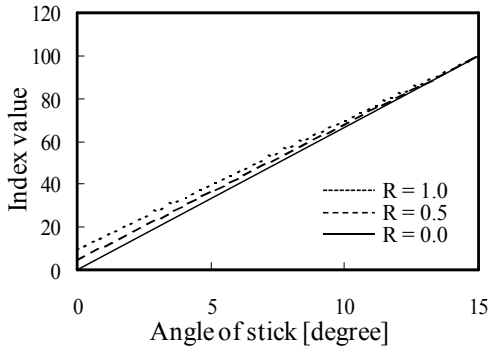

(b) Rise-to-Peak time-type index

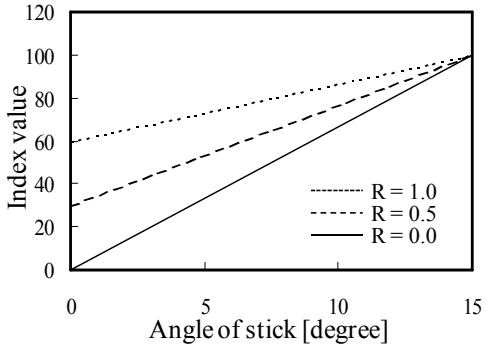

(c) Echo amplitude-type index

Figure 5.4 The relationships between the probe angle and the value of the angle indexes. (a) Ideal index. (b) Rise-to-Peak time-type index. (c) Echo amplitude-type index.

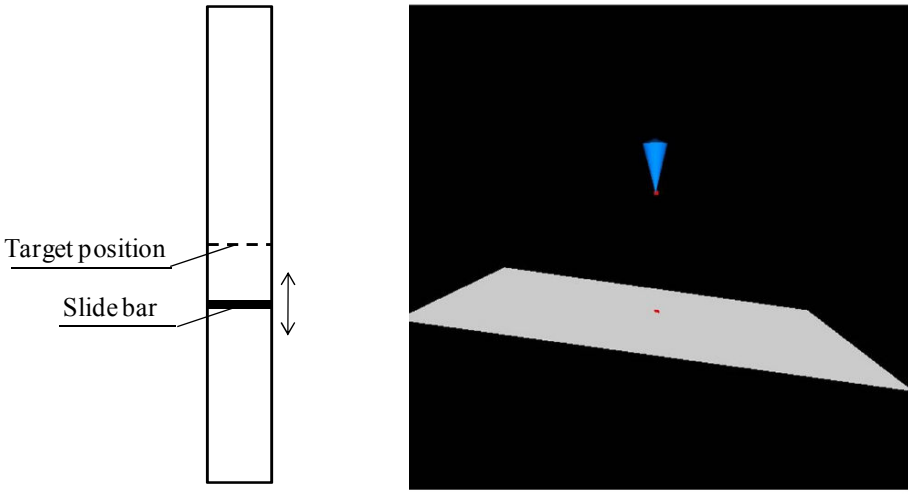

(a) Presentation of the distance between stick and imaginary plane

(b) Image of the imaginary plane.

Figure 5.5 The users view on PC display. (a) The presentation of the distance between the stick and the imaginary plane using a slide bar. (b) The image of the imaginary plane.

Table 5.1 The order of the user test

	User 1-3	User 4-6	User 7-9
Ideal	1	3	2
Rise-to-Peak time-type	2	1	3
Echo amplitude-type	3	2	1

5.3 Result

Figure 5.6 shows the measured operation times. There were no significant differences between the indexes (Tukey's test, $p<0.05$). The final stick angle was significantly large for the case using the echo-amplitude type index compared with the Ideal index and the Rise-to-Peak time-type index as shown in Figure 5.7 (Tukey's test, $p<0.05$). Similarly, the stick moved strongly from the origin position in the case using the echo-amplitude type index compared with the Rise-to-Peak time-type index as shown in Figure 5.8 (Tukey's test, $p<0.05$).

The number of trials did not have a significant effect on the results (ANOVA, $p<0.05$).

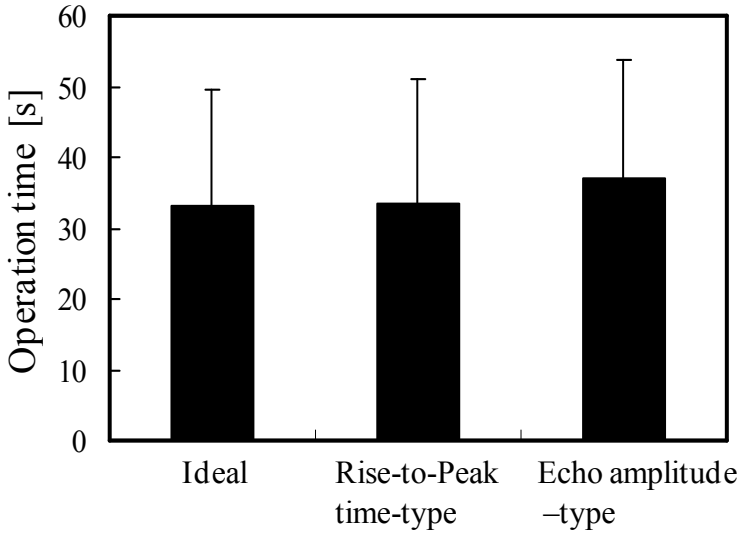

Figure 5.6 The operation times of the angle alignment task. Mean values (SD) are shown for the tasks using ideal index, Rise-to-Peak time-type and echo amplitude-type.

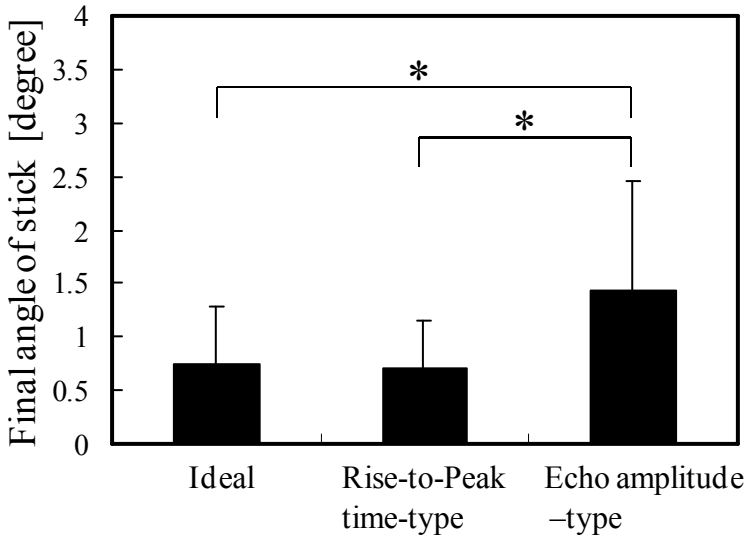

Figure 5.7 The final stick angle of the angle alignment task. Mean values (SD) are shown for the tasks using ideal index, Rise-to-Peak time-type and echo amplitude-type. * Significant difference by Tukey's test (P<0.05).

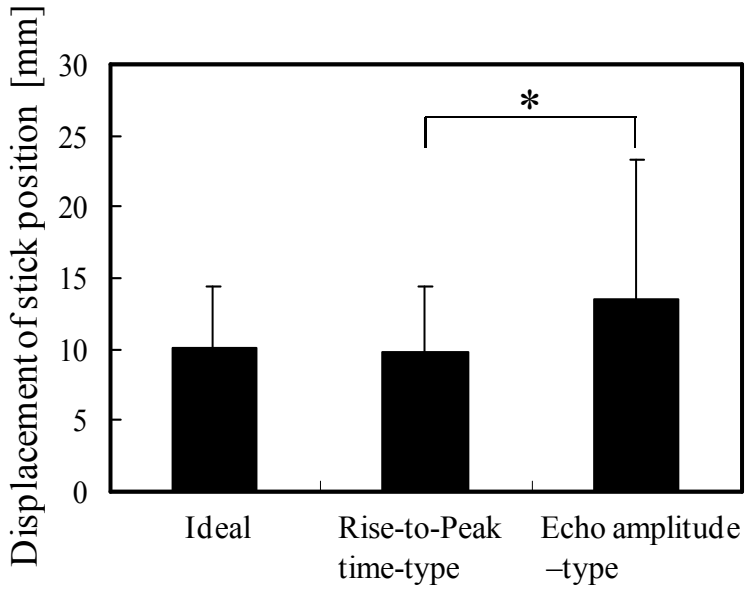

Figure 5.8 The displacement of the stick during the angle alignment task. Mean values (SD) are shown for the tasks using ideal index, Rise-to-Peak time-type and echo amplitude-type. * Significant difference by Tukey's test ($P<0.05$).

5.4 Discussion

The previous study reported that the change of surface roughness of articular cartilage could decrease the variation width of the echo amplitude caused by the change of the probe angle by 60% [2, 3]. Meanwhile, the decrease in the variation width of the Rise-to-Peak time was only 10%. From this characteristic of not being affected by the disturbance, it was predicted that the display of the Rise-to-Peak time can decrease the measurement time and the displacement of the ultrasound probe compared with using the echo amplitude as the angle index.

In this study, the user test, which imitates ultrasound measurement, was performed to evaluate the effectiveness of the Rise-to-Peak time. As expected in the previous study, the use of an index that is little affected by disturbance provides accurate angle alignment and suppression of the displacement. However, the use of an index that is little affected by disturbance did not decrease the operation time. Also, as shown in Figure 5.9, not only the movement in the direction where the surface roughness parameter changes but also the movement in the direction where the surface roughness parameter does not change was decreased by the use of Rise-to-Peak time-type index. This result suggests that the mapping of the stick state to the cognitive space of the user was improved by using a Rise-to-Peak time-type index.

In the clinical operation, the operator's visual resource was used for getting most of the information, such as the arthroscopic image, the surgical instrument, and the condition of the patient. Wickens insisted that the information processing performance is improved by assigning a part of the information to the auditory resource in tasks where the operator is overloaded by visual input [4]. Therefore, in this study, the angle indexes were presented as auditory feedback. However, because there are some other

sounds in the operation site such as electrocardiograms or air-conditioning equipment, and because the parameter mapping of the auditory feedback affects the information processing [5, 6], further study in designing the auditory feedback system is required for effective angle presentation in the clinical setting.

In conclusion, the effectiveness of the Rise-to-peak time during angle alignment was evaluated by a user test. From the results, the use of a Rise-to-Peak time-type index provides accurate angle alignment and suppression of probe displacement. It suggests that the use of a Rise-to-Peak time enables the accurate evaluation of articular cartilage in clinical use. However, study into how to present auditory feedback to the user in order to make the presentation of the Rise-to-Peak time more effective is still necessary.

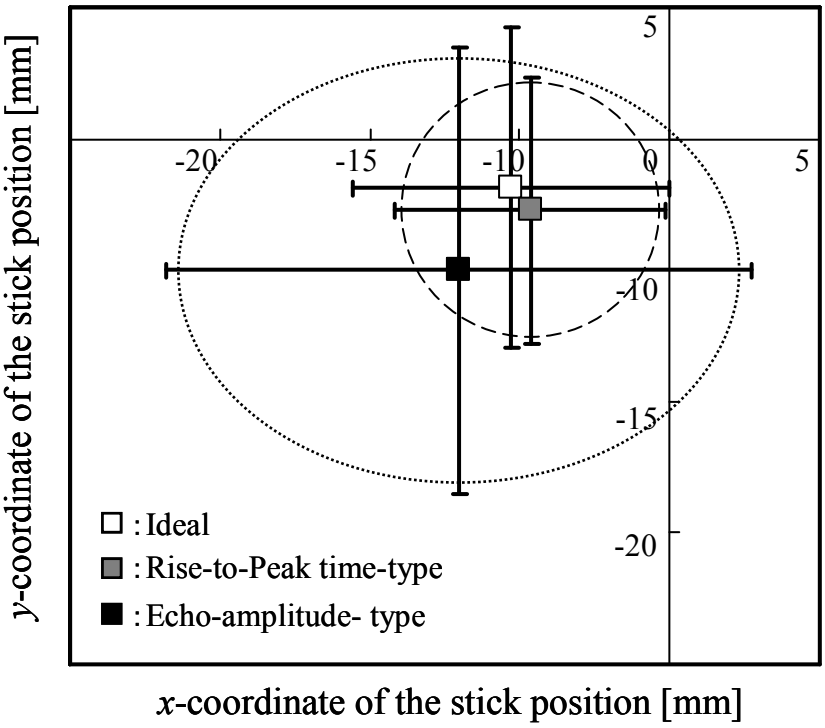

Figure 5.9 The final stick potion of the angle alignment task. Mean (SD) values of the *x*-coordinate and the *y*-coordinate of the final stick position are shown for the tasks using ideal index, Rise-to-Peak time-type and echo amplitude-type.

5.5 Reference

[1] Yamada, K., Oda, K., Tomita, N, Measurement of probe angle for ultrasound evaluation of articular cartilage using “Rise-to-Peak time”, Journal of Biomechanical Science and Engineering, Vol.5, (2010), pp. 615-624

[2] Yamada, K., Oda, K., Tomita, N, Effectiveness of Using the “Rise-to-Peak time” Index as a Guide for Ultrasound Evaluation of Articular Cartilage, Journal of Biomechanical Science and Engineering, *in preparation*

[3] Minns, R.J., Steven, F.S., The collagen fibril organization in human articular cartilage. Journal of Anatomy, Vol. 123, (1977), pp. 437-457

[4] Wickens, C.D., Processing resources in attention. (R. Parasuraman & D.R. Davies, eds.), Varieties of Attention, Academic Press, (1984)

[5] Walker, B.N., Kramer, G., Mappings and metaphors in auditory displays: An experimental assessment, ACM Transactions on Applied Perception, Vol. 2, (2005), pp. 407-412

[6] Neuhoff, J.G., Kramer, G., Wayand, J., Pitch and loudness interact in auditory displays: Can the data get lost in the map?, Journal of Experimental Psychology, Vol. 8, (2002), pp. 17-25

Chapter 6

Evaluation of Anisotropic Structure of Articular Cartilage Using Surface Acoustic Wave

6.1 Introduction

Articular cartilage is anisotropic with respect to elasticity, lubrication, and collagen fiber structure [1-5]. If regenerated cartilage does not have the same anisotropic structure as the host cartilage, it is possible that degeneration and destruction of the cartilage can occur due to stress concentration at the interface between the intact cartilage and regenerated cartilage. Therefore evaluation of the anisotropy of the cartilage is required as one of the indexes for the evaluation of regenerated cartilage. However, current methods to evaluate the anisotropy of articular cartilage, like microscope observation, split-line, or friction test, are destructive, with no nondestructive method having been established.

The aim of this study is to investigate the effectiveness of the measurement of shear wave speed using the surface wave as a first step in the development of a nondestructive method to evaluate the anisotropy of articular cartilage.

6.2 Material and method

6.2.1 Preparation of cartilage samples

Articular cartilage with subchondral bone were excised from the patellar surface, the medial condyle of the femur and the lateral condyle of the femur from porcine knee joints.

6.2.2 Measurement of shear wave speed using surface wave

Figure 6.1 shows the schematic diagram of the measurement system. The system consisted of an XY stage, a bimorph transducer, a function generator, an oscilloscope and a laser Doppler vibrometer. The sample was fixed on the XY stage with the cartilage side up.

The surface wave (6.0 kHz) was produced on cartilage surface by the bimorph transducer, and the vibration of the cartilage surface was measured by laser Doppler vibrometer at points of 5 mm and 10 mm away from the vibration excitation point. Figure 6.2 shows a typical measured waveform of a surface wave. The 6.0 kHz wave was extracted from the measured waveform using a wavelet transformation. The surface wave phase velocity was measured from the difference between the wave arrival times at the two measurement points of the vibrometer. This measurement of the surface wave phase velocity was performed in the directions parallel and perpendicular to the direction of joint movement. Also, the cartilage thickness of the measurement point was measured with the ultrasound measurement described in chapter 2 (typical waveform was shown in Figure 6.3). In this study, 1600 m/s was used as the speed of sound. The speed of the shear wave in cartilage was calculated from measured surface

wave phase velocity and cartilage thickness under the assumption that the surface wave is an air-coupled Rayleigh wave [6].

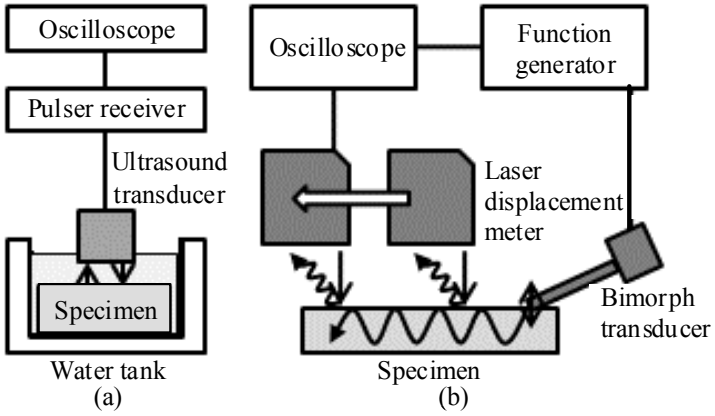

Figure 6.1 Schematic diagram of ultrasound measurement system. (a) Measurement of the cartilage thickness using longitudinal wave. (b) Measurement of the speed of the shear wave using surface wave.

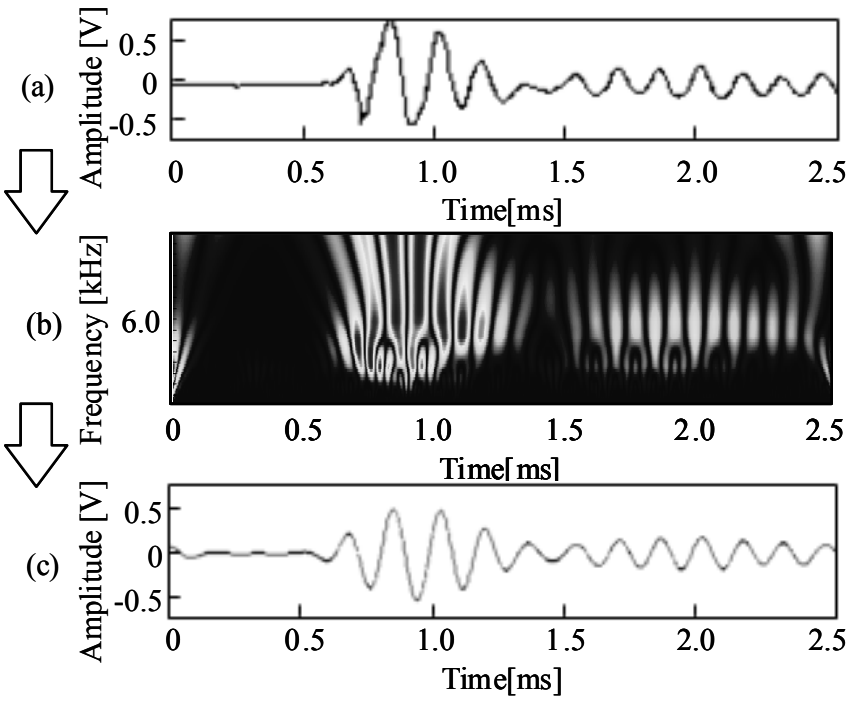

Figure 6.2 Wavelet-transform analysis. (a) Measured waveform of the surface wave. (b) Wavelet map. (c) Result of extraction. Frequency = 6.0 kHz.

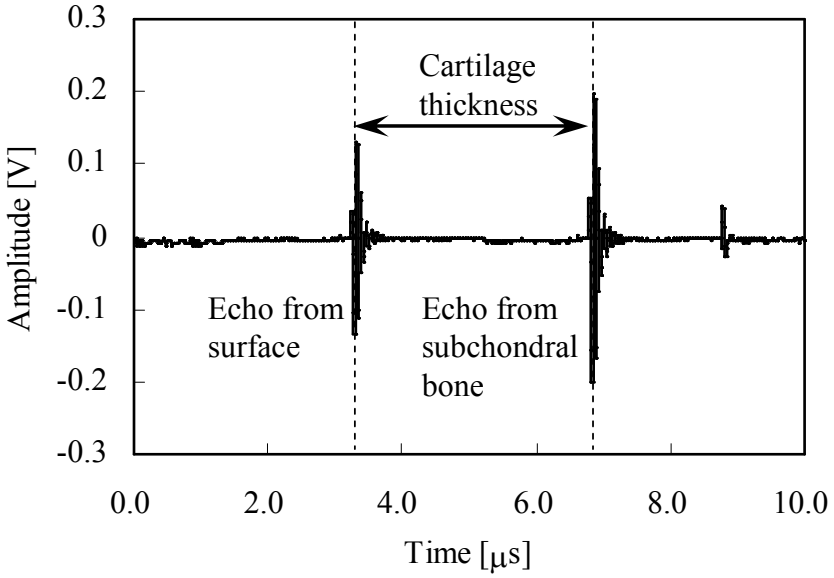

Figure 6.3 Typical waveform of the ultrasound echo (Frequency = 10 MHz). Echoes from the surface and the bottom of the specimen were observed.

6.2.3 Observation of split-line

The split-line was created by inserting a needle at a 90° angle (to the joint surface) into the articular cartilage to the level of the subchondral bone. Before the insertion, the needle was dipped in ink, which stained the exposed cartilaginous matrix, making the split-lines clearly visible. This procedure was repeated at 1mm intervals in a grid pattern until the entire specimen surface was mapped. The image of the split-line was binarized and ellipse approximation was performed. As shown in Figure 6.4, the angle of split-line extension was defined as the angle between the direction of joint movement and the major axis of the ellipse.

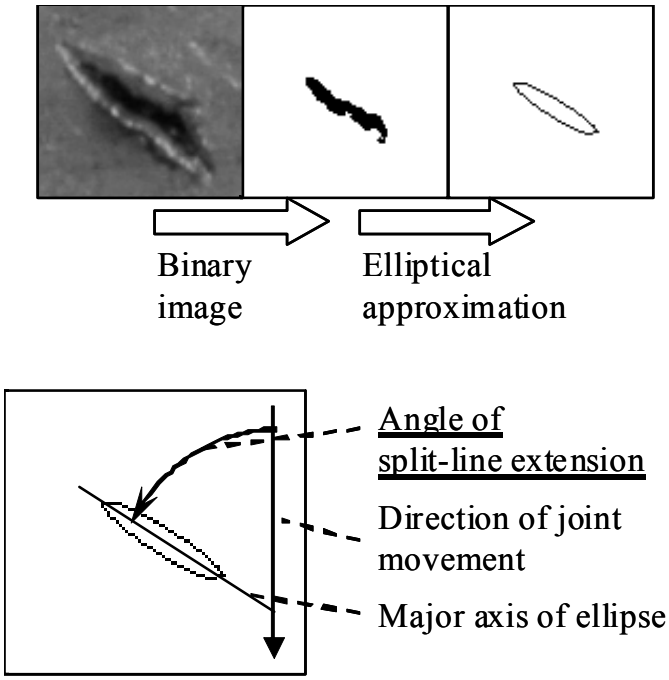

Figure 6.4 Measurement of the split-line extension angle. The angle was defined as the angle between the direction of joint movement and the major axis of the ellipse.

6.3 Result

Figure 6.5 shows the speed of the shear wave in the patellar surface and the condyle of the femur. In the patellar surface, the speed of the shear wave measured in the direction parallel to the joint movement was significantly lower than that for the perpendicular direction ($p<0.05$). Meanwhile, in the condyle of the femur, although the same tendency was observed in the lateral condyle of the femur, a significant difference in the speed of the shear wave was not observed between the parallel direction and the perpendicular direction (Figure 6.6).

Figure 6.7 shows the split-line in the 5x5 [mm] area where surface wave measurement was performed. The direction of joint movement corresponds with the longitudinal direction of each photograph. In the patellar surface, the split-line tended to extend to the direction perpendicular to the direction of the joint movement. Meanwhile, in the condyle of the femur, the split-line extended diagonally to the direction of the joint movement.

Figure 6.8 shows the average angles of split-line extension. The average angles were 90° (SD 20) in the patellar surface, and 60° (SD 10) in the condyle of the femur.

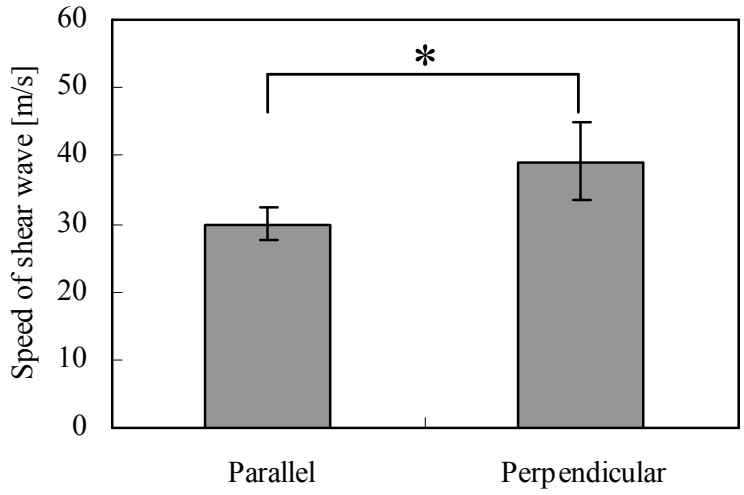

Figure 6.5 Speed of the shear waves in the patellar surface. Mean values (SD) are shown for each direction of wave propagation. * Significant difference by Student's t-test ($P<0.05$).

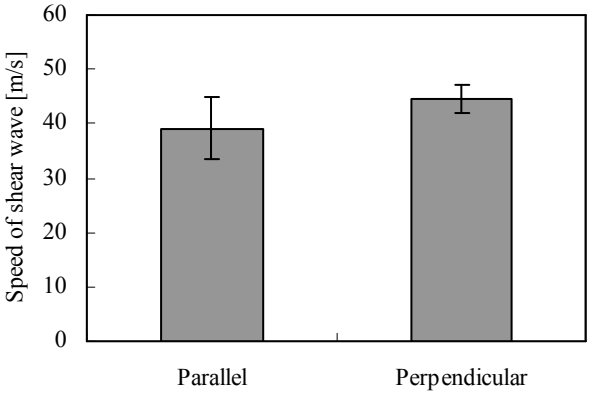

(a) Lateral condyle of femur

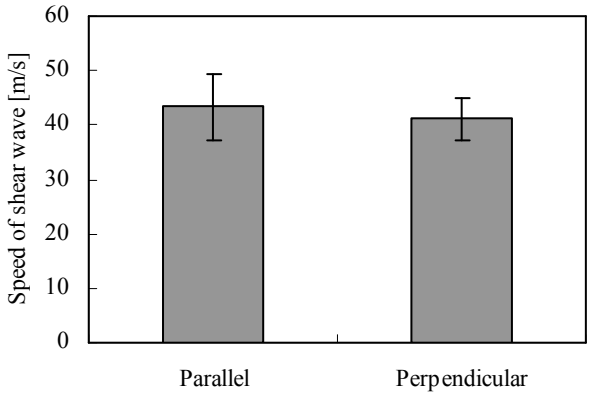

(b) Medial condyle of femur

Figure 6.6 Speed of shear waves in the condyle of the femur. (a) Lateral condyle of the femur. (b) Medial condyle of the femur. Mean values (SD) are shown for each direction of wave propagation. * Significant difference by Student's t-test (P<0.05).

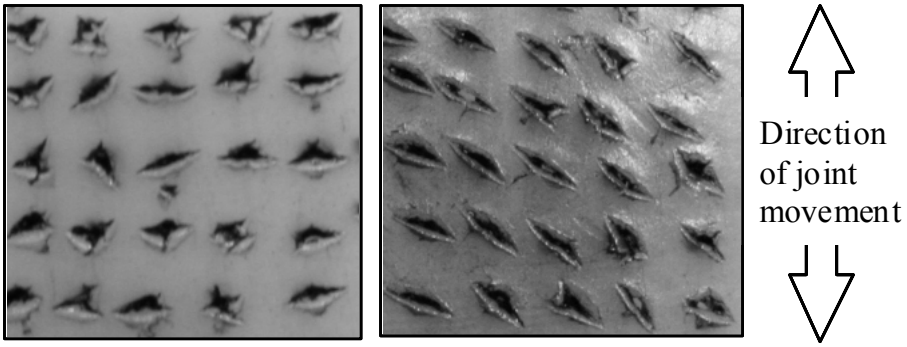

(a) Patellar surface (b) Condyle of femur

Figure 6.7 Photographs of the created split-lines on the cartilage surface. (a) Patellar surface. (b) Condyle of the femur. Direction of joint movement corresponds with the longitudinal direction of each photograph.

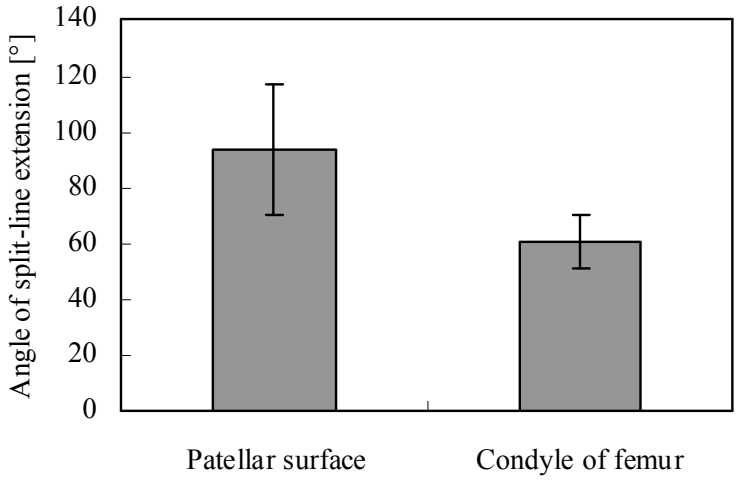

Figure 6.8 Angle of split-line extension. Mean values (SD) are shown for patellar surface and for the condyle of the femur.

6.4 Discussion

Roth et al. evaluated the elasticity of articular cartilage by tensile test, and reported that the tensile force is high in the direction parallel to the split-line extension and low in the direction perpendicular to the split-line. Ikeuchi et al. reported that the lubrication property of articular cartilage has anisotropy related to the direction of joint movement.

In this study, the speed of the shear wave that propagates parallel and perpendicular to the direction of joint movement was measured. In the patellar surface, the speed of the shear wave measured in the direction parallel to the joint movement was significantly lower than that measured in the perpendicular direction. In the lateral condyle of the femur, the same tendency was observed. Meanwhile, in the medial condyle of the femur, this phenomenon wave was not observed. Because the speed of a shear wave is affected by the shear modulus of the medium, it is possible that the observed anisotropy of the speed of the shear wave reflects the anisotropy of shear modulus of the cartilage and the anisotropy of the orientation of collagen fibers that sustains the elastic modulus of the articular cartilage [7].

Although the difference in the anisotropies of the cartilage structure in the patellar surface and the condyle of the femur is not clear, it is thought that the structural and mechanical characteristics of the cartilage are developed with cartilage maturation via mechanical stimulus [8]. As shown in Figure 6.9, the relative sliding motion caused by the bending of the knee is in constant direction along the patellar surface. In the condyle of the femur, the relative sliding motion is comparatively multidirectional because of the medial rotation and lateral rotation of the tibia. Also, the sliding motion

is more multidirectional in the medial condyle of the femur compared with the lateral condyle of the femur. This difference in the sliding history for each site might construct the difference in the cartilage structure. Therefore it is suggested that the anisotropy of the speed of the shear wave reflected the anisotropy of the cartilage structure constructed by the sliding stimulus. In addition, the direction of the split-line extension, which corresponds to the direction of the collagen fibers [9], shows correlation with the direction in which the speed of the shear wave is high in the patellar surface.

Because the residual stress of articular cartilage might also affect the extension of split-line angle and the speed of the shear wave, a study considering nonlinear characteristics of cartilage is required for investigating what is reflected in the speed of the shear wave.

In conclusion, the availability of measuring the shear wave speed as a nondestructive method to evaluate the anisotropy of articular cartilage was evaluated. From the results, an anisotropy of the speed of the shear wave was observed for areas with different sliding motion histories. These results suggest that the structural and mechanical anisotropy of cartilage can be evaluated by the measurement of shear wave speed. A study to investigate what structure is reflected in the speed of the shear wave, and a reduction in size for the measurement device are required before clinical use can begin.

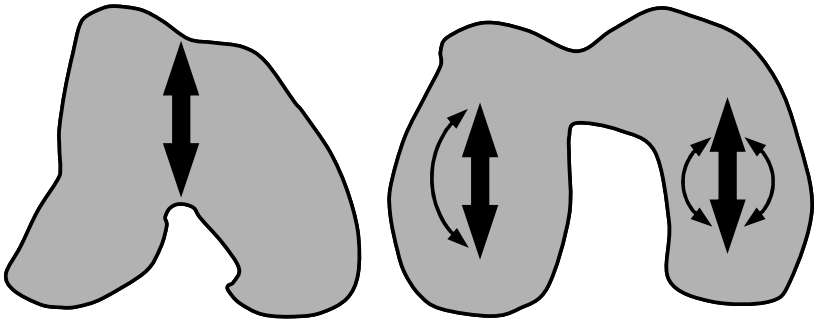

Figure 6.9 Direction of relative slip. (a) Patellar surface. Anterior view of the femoral head. (b) Condyle of the femur. Inferior view of the femoral head.

6.5 Reference

[1] Huang, C.Y., Stankiewicz, A., Ateshiana, G.A., Mow, V.C., Anisotropy, inhomogeneity, andtension–compression nonlinearity of human glenohumeral cartilage in finite deformation, Journal of Biomechanics, Vol. 38, (2005), pp. 799-809

[2] Ikeuchi, K., Shibata, N., Arimoto, M., Tomita, N., Cottle, W., Friction between articular cartilage and meniscus in the knee joint, Japanese Journal of Clinical Biomechanics, Vol. 15, (1994), pp. 183-186

[3] Roth, V., Mow, V.C., The intrinsic tensile behavior of the matrix of bovine articular cartilage and its variation with age, Journal of Bone and Joint Surgery, Vol. 62, (1980), pp. 1102-1117

[4] Chahine, N.O., Wang, C.B., Hung, C.T., Ateshian, G.A., Anisotropic strain-dependent material properties of bovine articular cartilage in the transitional range from tension to compression, Journal of Biomechanics, Vol. 37, (2004), pp. 1251-1261

[5] Jeffery, A.K., Blunn, G.W., Archer, C.W., Bentley, G., Three-dimensional collagen architecture in bovine articular cartilage, Journal of Bone and Joint Surgery, Vol. 73, (1991), pp. 795-801

[6] Sato, Y., The theory of elastic undulation, Iwanami Shoten, Publishers, (1978), pp. 97-102

[7] Zhu, W., Mow, V.C., Koob, T.J., Eyre, D.R., Viscoelastic shear properties of articular cartilage and the effects of glycosidase treatments, Journal of Orthopedic Research, Vol. 11, (1993) pp. 771-781

[8] Roth, V., Mow, V.C., The intrinsic tensile behavior of the matrix of bovine articular cartilage and its variation with age, The Journal of Bone and Joint Surgery, Vol. 62, (1980), pp. 1102-1117

[9] Below, S., Arnoczky, S.P., Dodds, J., Kooima, C., Walter, N., The split-line pattern of the distal femur: a consideration in the orientation of autologous cartilage grafts, Journal of Arthroscopic and Related Surgery, Vol. 18, (2002), pp. 613- 617

List of Publications

[1] Yamada, K., Ikeuchi, K., Hattori, K., Tomita, N., Correction of thickness measurement by ultrasound for articular cartilage using sound velocity estimation, Journal of Biomechanical Science and Engineering, Vol.5, no.2, (2010), pp. 175-184

[2] Yamada, K., Yamamoto, K., Tomita, N, Evaluation of anisotropic structure of articular cartilage using surface acoustic wave, IEICE Technical Report, vol.109, no.388, (2010), pp. 1-4 (in Japanese)

[3] Yamada, K., Oda, K., Tomita, N, Measurement of probe angle for ultrasound evaluation of articular cartilage using “Rise-to-Peak time”, Journal of Biomechanical Science and Engineering, Vol.5, no.5, (2010), pp. 615-624

[4] Yamada, K., Oda, K., Tomita, N, Effectiveness of Using the “Rise-to-Peak time” Index as a Guide for Ultrasound Evaluation of Articular Cartilage, Journal of Biomechanical Science and Engineering, *in preparation*

謝辞

Acknowledgments

本研究は，京都大学大学院　工学研究科　機械理工学専攻　教授　富田　直秀　先生のご指導の下で実施されました．ここに厚く御礼申し上げると共に，深く感謝の意を表します．

椹木　哲夫　先生（京都大学大学院　工学研究科　機械理工学専攻　教授)には，学位論文審査の労をお執りいただきました．ここに深く感謝の意を表します．

玄　丞烋　先生（京都大学　再生医科学研究所　准教授)には，学位論文審査の労をお執りいただきました．ここに深く感謝の意を表します．

山本　健　先生（関西大学　システム理工学部　准教授）には，超音波計測と理論について多くのご助言を頂きました．ここに深く感謝の意を表します．

小田　浩平　氏（京都大学　富田研究室　学生），池田　隆之介　氏（京都大学　椹木研究室　学生)とは，本研究を共同で遂行させていただきました．ここに深く感謝の意を表します．

本論文，及び本研究を進めるにあたり，ご協力並びにご指導頂きました医療工学研究室の先輩，同級生，後輩の皆様に，深く御礼申し上げます．

最後に，私が博士課程後期課程に進学することに対して，理解を示し，温かく見守ってくれた両親・家族に感謝を表し，深く御礼申し上げます．

平成 23 年　2 月

山田　桂輔

DOCTORAL THESIS

博士(工学)　学位論文

Improving the Reliability of Ultrasound Evaluation of Articular Cartilage for Clinical Applications

関節軟骨超音波定量評価法の臨床使用を考慮した信頼性向上

Department of Mechanical Engineering and Science
Graduate School of Engineering
Kyoto University

京都大学大学院　工学研究科　機械理工学専攻

2011/2

Keisuke YAMADA
